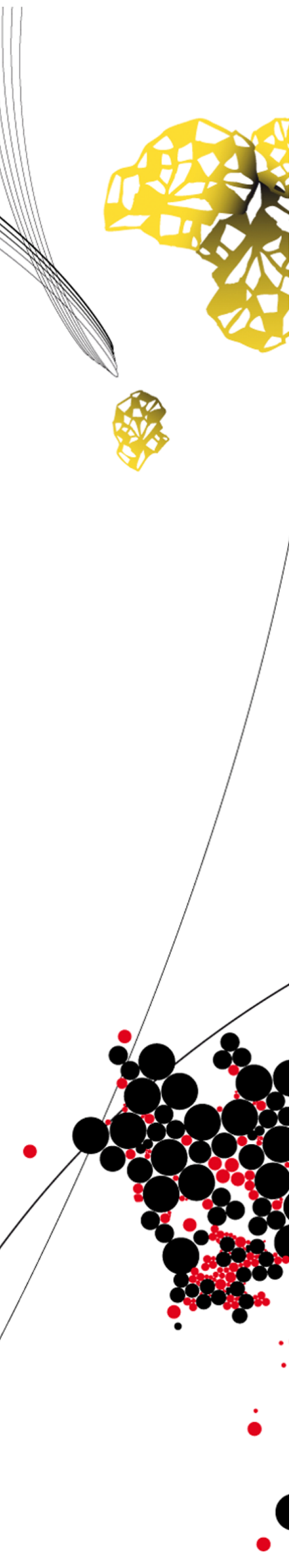

UNIVERSITY OF TWENTE.

Faculty of Electrical Engineering, Mathematics & Computer Science

Early Warning System for Safe Lateral Maneuver of Bicycles

Kaushik Kalaiselvan (s2276542)
MSc Embedded Systems
November 2021

Supervisors:
prof. dr. Paul Havinga
dr. ir. Yanqiu Huang
dr. ir. Andre Kokkeler

Faculty of Electrical Engineering,
Mathematics and Computer Science
University of Twente
P.O. Box 217
7500 AE Enschede
The Netherlands

Abstract

Sustainable and smart mobility strategies are now starting to be adopted to reduce the CO_2 emission as well as take advantage of digitalization and automation to achieve seamless, safe and efficient transportation. Bicycles and e-bikes are considered to be the leaders of this transition, as they are cost-effective and have a positive impact on health. With the growing popularity and usage of bicycles, cycling safety becomes more critical. Lateral maneuver of bicycles is a typically apprehended maneuver on the roads and improper assessment of the surroundings during this typically causes various accidents. Although, this action is highly similar to the lane change maneuver performed in cars, the assistance systems developed for cars will not be effective for bicycles, due to the characteristics traits of bicycles such as limited size/space, low cost, low weight, vehicle dynamics, and their road infrastructure. This brings many challenges to the system design. The solutions for bicycles are required to be cost effective, less complex in terms of hardware and software design, efficiently provide maximum utility with minimal resources, and provide a relatively good accuracy across different environments at the same time.

In this work, we design and demonstrate a novel multi-modal early warning system to assist cyclists in identifying dangerous situations during lateral maneuvers. To the best our knowledge, this is the first work that addresses the constraints, designs a complete system for lateral maneuver of bicycles and validates it using extensive experiments in real-road scenarios. It consists of a 76GHz millimeter wave (mmWave) radar sensor and two ultrasonic sensors to detect targets such as cars, trucks, bicycles and pedestrians in the rear-side blind spot regions as well as approaching from behind; and using the combination of Time-to-Collision (TTC) and Minimum-Safe-Distance (MSD) metrics to assess and generate warnings about potential danger at an early stage. The warnings generated by the system include two distinct information and provide improved utility towards the safety of bicycles. The warnings indicate the side of potential maneuvering hazard to host cyclist and of a dangerously approaching vehicle right behind the host bicycle. This additional information can be used to alert the cyclist of the approaching bicycle to be aware of the host bicycle to mitigate collision. From the extensive experiments in real-road scenarios, the method is deemed feasible and can identify threats and warns the rider about 5 seconds in advance with an accuracy of 95.2%.

Acknowledgement

I have successfully completed my research work, which was a part of my masters program under the smart bikes project group, of the Pervasive Systems chair. It also marks the end of my wonderful masters journey that began in September 2019.

I would like to express my sincere gratitude to my supervisor Yanqiu Huang, for guiding me throughout my thesis. Her technical inputs, feedback and support were of at most value to me and not only helped me to finish my work but also nurtured me for my future career. I would like to thank Deepak Yeleshetty, Akhil Pallamreddy, and Khalil Ben Fredj, who are pursuing their Phd under the smart bikes group at the University of Twente. Their participation in weekly meetings and discussion through the course of the project, helped me share my ideas and gain a better perspective. I also extend my gratitude to Paul Havinga and Andre Kokkeler for accepting to be part of my graduation committee.

Finally, I extend my gratitude to my family and friends for their constant support and motivation throughout the course of my masters journey. To my father, who has always been my inspiration to take up a technical career in the field of electronics. To my mother, who has been my pillar of support and source of motivation in periods of doubt, without whom this journey wouldn't have been possible. I also thank my friends Visshnu, Jegan, and Nithin for being with me throughout this incredible journey.

This masters program has been a wonderful experience and has enabled me to experience life away from home. This is an experience that will be most valuable to me in terms of academics and life. I thank the University of Twente for presenting me with this opportunity.

Contents

Abstract **1**

Acknowledgement **2**

List of Acronyms **5**

1 Introduction **10**
1.1 Objective . . . 13
1.2 Contribution . . . 13

2 System Requirements **15**
2.1 Surrounding Information Extraction . . . 15
2.2 Threat Assessment . . . 17
2.3 Response . . . 17

3 State-of-the-Art and Critical Analysis **18**
3.1 Surrounding Information Extraction . . . 18
3.1.1 Vision Based Sensors . . . 18
3.1.2 Non-Vision Based Sensors . . . 19
3.1.3 Vehicular Communication . . . 23
3.1.4 Sensor Fusion . . . 24
3.1.5 Comparison of SoA methods . . . 24
3.2 Threat Assessment Methods . . . 25
3.2.1 Deterministic Method . . . 25
3.2.2 Probabilistic Method . . . 26
3.2.3 Comparison of SoA Methods . . . 27
3.3 Response . . . 28
3.3.1 Intervening Type . . . 28
3.3.2 Warning Type . . . 28
3.3.3 Comparison of SoA Methods . . . 28
3.4 Summary . . . 28

4 Theory and Background **30**
4.1 Fundamentals of Frequency Modulated Continuous Wave (FMCW) Radar 30
4.2 Range Estimation . . . 31
4.3 Velocity Estimation . . . 32
4.4 Angle Estimation . . . 33

5 Proposed Early Warning System For Safe Lateral Maneuver of Bicycles **34**
5.1 System Overview . . . 35
5.1.1 Hardware Overview . . . 36
5.1.2 Software Overview . . . 36
5.2 Functional Blocks Realization . . . 38
5.2.1 Surrounding Vehicle Information Extraction . . . 38
5.2.2 Threat Assessment . . . 48
5.2.3 Warning Algorithm . . . 49

6 Testing and Results **51**
6.1 Ultrasonic Sensor Performance . . . 51
6.2 mmWave Radar Performance . . . 53
6.2.1 Detection Range in Different Road Scenarios: . . . 53
6.2.2 Accuracy of the Millimeter Wave (mmWave) Radar: . . . 55
6.3 Lateral Maneuver Warning System . . . 56
6.3.1 ISO 17387 Testing Procedure: . . . 56
6.3.2 Real-time Scenario Testing: . . . 57
6.4 Limitations . . . 61

7 Conclusion **63**
7.1 Future Work . . . 63

List of Acronyms

ADAS	Advanced Driver Assistance Systems
ADC	Analog-to-Digital Converter
B2V	Bicycle-to-Vehicle
CA	Cell Averaging
CAN	Controller Area Network
CASO	Cell Averaging Smallest Of
CFAR	Constant False Alarm Rate
DBSCAN	Density Based Spatial Clustering of Applications with Noise
DSP	Digital Signal Processor
DST	Deceleration-to-Safety-Time
e-bikes	Electric Bikes
FFT	Fast Fourier Transform
FMCW	Frequency Modulated Continuous Wave
FN	False Negative
FoV	Field of View
FP	False Positive
GND	Ground
GPIO	General Purpose Input Output
GUI	Graphical User Interface
IF	Intermediate Frequency
LCDAS	Lane Change Decision Aid Systems
LIDAR	Light Detection and Ranging

MCU	Micro Controller Unit
mmWave	Millimeter Wave
MSD	Minimum Safe Distance
RADAR	Radio Detection and Ranging
RCS	Radar Cross Section
RF	Radio Frequency
RX	Receiver
SDK	Software Development Kit
SNR	Signal to Noise Ratio
SoA	State-of-the-Art
THW	Time-Headway
TN	True Negative
TP	True Positive
TTB	Time-to-Brake
TTC	Time-to-Collision
TX	Transmitter
UART	Universal Asynchronous Receiver Transmitter
Vcc	Power
V2B	Vehicle-to-Bicycle
V2I	Vehicle-to-Road Infrastructure
V2V	Vehicle-to-Vehicle

List of Figures

1.1 Fatal and Serious Injuries by Mode of Travel [4] . . . 10
1.2 Driver Responsibility in Advanced Driver Assistance Systems (ADAS) [7] 11
1.3 High-risk Lateral Maneuver Scenarios . . . 12

2.1 System Functional Blocks . . . 15

3.1 Ultrasonic Sensor Working [23] . . . 20
3.2 Acoustic Detector Working . . . 20
3.3 Radar Sensor Working . . . 21
3.4 Radar Operation Bands . . . 21
3.5 Lidar Sensor Working . . . 23
3.6 Vehicular Communication Working [47] . . . 24

4.1 FMCW Radar Working . . . 30
4.2 Range Estimation Principle [60] . . . 31
4.3 Velocity Estimation Principle . . . 32
4.4 Angle Estimation Principle . . . 33
4.5 Angle Estimation Accuracy . . . 33

5.1 System State Diagram . . . 34
5.2 System Overview . . . 35
5.3 Hardware Implementation Block Diagram . . . 36
5.4 Software Flow Chart . . . 37
5.5 System sensor coverage . . . 38
5.6 HC-SR04 Ultrasonic Sensor [61] . . . 39
5.7 IWR1642 BOOST EVM [62] . . . 40
5.8 Radar Front-end . . . 41
5.9 Radar Tx Frame . . . 43
5.10 Radar Back-end Processing Chain . . . 44
5.11 Range Vs SNR . . . 45
5.12 Radar Output Frame . . . 48
5.13 Threat Assessment Method . . . 48
5.14 Warning Algorithm . . . 50
5.15 Closing Target Virtual Direction Separation . . . 50

6.1 System Mounting on Bicycle . . . 51
6.2 Ultrasonic Sensor Field Trial Setup . . . 52
6.3 Ultrasonic Sensor Measurement Analysis . . . 52
6.4 mmWave Radar Visualization Screen . . . 53
6.5 Road Scenarios . . . 54

6.6 Detection Range Plot 55
6.7 Radar Accuracy 56
6.8 Test Scenarios 56
6.9 Early Warning Timings 61

List of Tables

3.1 Non-Vision Based Information Extraction SoA Methods Comparison . . . 25
3.2 Deterministic Approach Metrics Comparison . . . 27

5.1 Radar front-end configuration . . . 42
5.2 Constant False Alarm Rate (CFAR) - Configuration . . . 44
5.3 Maximum Range Parameters . . . 45
5.4 Range Based Pruning . . . 46
5.5 DBSCAN - Configuration . . . 47

6.1 ISO 17387 Testing results . . . 57
6.2 Performance Evaluation Metrics . . . 58
6.3 Confusion Matrix - Noisy Road Scenarios . . . 59
6.4 Confusion Matrix - Dedicated Bicycle Lane Scenario . . . 59
6.5 Performance Metrics - Individual Scenario . . . 60
6.6 Confusion Matrix - Overall Performance . . . 60
6.7 Performance Metrics - Overall System . . . 60

Chapter 1

Introduction

In the current era, the world is moving towards a smarter and sustainable tomorrow. According to the United Nations Regional Information Centre (Western Europe), mobility is considered to be one of the most essential elements of the development strategies that aim to achieve the sustainable development goals [1]. While mobility offers its users many benefits, it does not come without consequences to our society. Negative effects such as greenhouse gas emissions, air and water pollution, noise pollution, congestion, along with road accidents, affect our health and well-being. The transportation sector is seen to be responsible for 24% of the global CO_2 emissions [2]. Thus, new sustainable and smart mobility strategies are now starting to be adopted to reduce the CO_2 emission as well as take advantage of digitalization and automation to achieve seamless, safe, and efficient transportation. This has resulted in conventional vehicles becoming more advanced and the rise in popularity of non-emitting transportation such as bicycles, electric cars, and Electric Bikes (e-bikes). Bicycles and e-bikes are considered to be the leaders of this transition as they are cost-effective and have a positive impact on health. The bicycle industry is transforming, significant growth is being seen in both sales and production of bicycles especially e-bikes and is forecast to grow up to 30 million sales per year across Europe by 2030 [3].

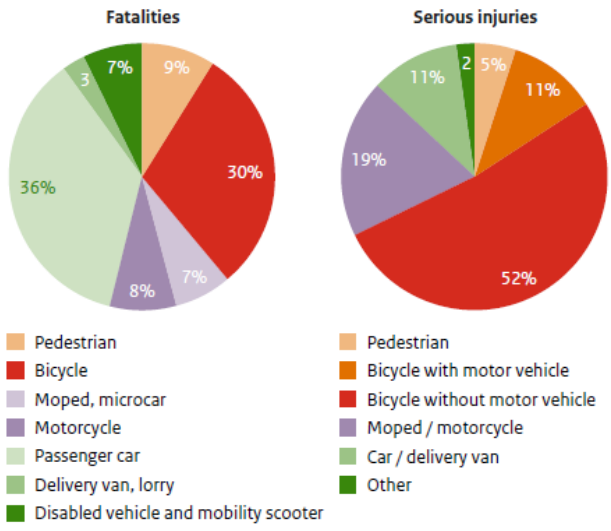

Figure 1.1: Fatal and Serious Injuries by Mode of Travel [4]

The increase in the number of bicycles with higher speeds might also increase the number of accidents that may occur. In 2016, 30% of the road accident deaths involved cyclists and e-cyclists as shown in Fig. 1.1. According to the analysis conducted by Statistics Netherlands, the number of traffic accident deaths over the past two decades (1999 to 2019) in car occupants is seen to have dropped by 60%, while it is only 11% among cyclists [5]. Despite extensive cycling infrastructure in The Netherlands, it has the second most cyclists death rate in Europe due to the commonness of cycling [6]. These data support the fact that there is a lot of focus on the safety of high-end automobiles with the implementation of many advanced technologies. There is ongoing work in the direction of ADAS technologies that are focused towards coordinated and autonomous driving. Whereas very minimal attention has been directed towards the safety of bicycles. The number of accidents involving bicycles is very high, which demands more research attention due to their increasing popularity and their capability to become the major mode of transportation for a smart and sustainable future.

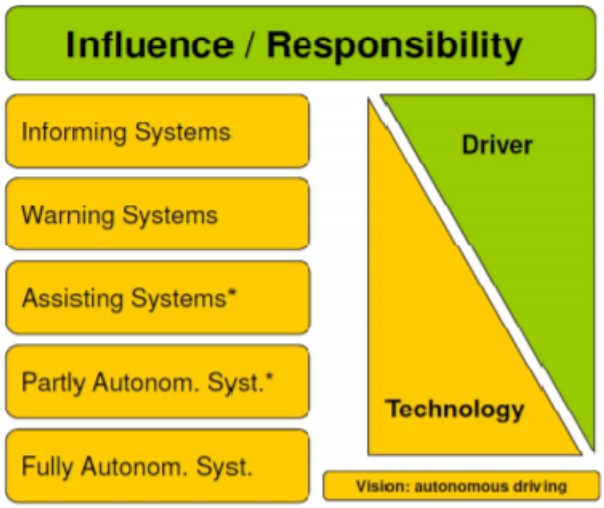

Figure 1.2: Driver Responsibility in ADAS [7]

According to statistical reports, human errors are seen to account for 90% of traffic accidents [8]. The main goal of ADAS is to mitigate human errors during driving by assisting the driver in a variety of ways. These systems interact with the driver and require the engagement of the driver. Simple ADAS only provide vital monitoring information of the surroundings to the driver, whereas with advancements they can also provide guidance and take control during certain simple scenarios in some class of vehicles as shown in Fig. 1.2. ADAS is a term that originated from automobile driving and is focused on high-end vehicles [7], with currently increasing ADAS features and built towards automated driving. A wide range of assistance systems has been implemented for different vehicles such as cars, trucks, and bicycles with different technologies and functionalities. Each system is found to contribute to safety through different means with its own benefits and drawbacks. The increased scientific attention of such systems for cars has also led to significant commercialization.

The most important ADAS features that have been implemented in cars are inferred to be:

- Forward collision warning and mitigation.
- Closing vehicle warning.
- Blind-spot warning.
- Lane change assistance.

Lane changing is a typically apprehended maneuver on the roads and requires careful assessment of the surrounding vehicles to preclude any risk of the maneuver to other road users before execution. It has a high error potential and is one of the main causes of various severe crash accidents [9]. The Lane Change Decision Aid Systems (LCDAS) combines the functioning of blind-spot and closing vehicle warning systems. There is a wide range of ADAS for lane change assistance available and are developed for cars. Some of these systems only aid in the better decision of the driver during lane change, while others execute the maneuver end-to-end [10] [11] [12] [13] [14] [15]. The focus on cars has resulted in complex and expensive systems. The assistance system developed for bicycles is very minimal and is mostly focused on providing closing vehicle warnings [16] [17] [18]. Despite the lack of clear lane separation in most scenarios, lateral maneuvers similar to lane changing are performed by cyclists, within the dedicated bicycle lane or in a shared road infrastructure without a dedicated bicycle lane. The cyclists are required to perform a similar kind of action performed by drivers in cars during lane change maneuvers during the process of lateral maneuvers. The cyclist must turn back and look for any vehicle on the adjacent side as well as approaching from behind and assess its attributes such as speed and distance to make the decision of performing the maneuver in that direction. This action may have a detrimental influence on safety since the cyclist will be unable to focus on the path in front during the scanning process. It may also cause the cyclist to drift to the side, which may result in an accident. In addition, the tendency of the cyclist to improperly assess the surroundings and underestimate the speed of distant approach vehicles from behind is also common. These factors contribute to the reduction of safety and increase the possibility of collision during lateral maneuvers. The Fig. 1.3 depicts some scenarios in which the lateral maneuvers are inferred to be dangerous.

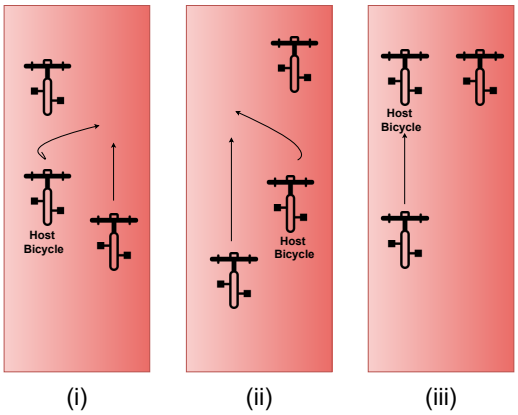

Figure 1.3: High-risk Lateral Maneuver Scenarios

1.1 Objective

Bicycles are very different from high-end automobiles such as cars, in several aspects. They are a low-end transportation mode with a long, narrow, and lightweight body with a different road infrastructure from cars. These characteristics traits have a very crucial role in the type of technological solutions that are designed for them. The solutions are required to be cost-effective, less complex in terms of hardware and software design, efficiently provide maximum utility with minimal resources, and provide relatively good accuracy at the same time. Thus, solutions that have been developed for cars and other high-end vehicles will not be effective for bicycles. Considering all these factors the goal of this thesis is to **'Design an early warning system for safe lateral maneuver of bicycles'**.

The key sub-questions that are addressed in this thesis are:

- What is the suitable sensor technology for bicycles to effectively collect the surrounding vehicle information?
- How to design a simple and effective warning algorithm suitable for bicycles using the suitable sensors?
- What is the performance of the designed warning system under real-road scenarios?

1.2 Contribution

In this chapter, the brief background information on the trend of bicycle usage was provided to highlight the importance of the current research domain which is focused on the safety of bicycles. Then a detailed motivation was provided for deciding to design a warning system for safe lateral maneuver of bicycles followed by the objectives and the goals of the research. The solutions of the sub-questions listed above are then covered in chapters 3 to 5, as indicated in Section 1.1 . Finally, the conclusion and future work of this project are presented in Chapter 7. The main contribution of this work can be summarized as follows:

- A complete system for lateral maneuver of bicycles addressing the constraints using low-cost off-the-shelf components, including a mmWave radar sensor, two ultrasonic sensors, and a Raspberry Pi, to detect both short-range and long-range hazards is designed.
- By carefully configuring the TX signal in the front-end and removing redundant reflection points using the back-end processing, the mmWave radar achieves maximum range and velocity detection of each interested target with minimal power and computational complexity. This guarantees the system is feasible for a low-end vehicle and can generate on-time warnings.
- An improved deterministic-based algorithm is proposed for bicycles to assess the lateral maneuver threat in a human-like manner using a combination of Time-to-Collision (TTC) and Minimum Safe Distance (MSD) metrics. It reduces false positives with low computational complexity.

- An improved warning algorithm for bicycles that includes two information, one for the sides and one for the straight is designed. This functionality is expected to improve safety by also preventing possible rear collisions even in an environment where the other bicycles are not equipped with the same assistance system. This is inferred to improve the utility of the system and contribute more to the safety of bicycles.

- Extensive field tests are carried out to evaluate the performance and accuracy of sensors in real outdoor environments. The warning system accuracy of 95.2% and an early warning time of 5 secs for different real road scenarios and lighting conditions was achieved. This proves the effectiveness and robustness of the system.

Chapter 2

System Requirements

In this chapter, a general introduction to understanding the main functional blocks of the assistance system along with their requirements is given. The requirements of each functional block based on the system requirements mentioned in Section 1.1 is provided to help correspond to the comparison metrics used for analysis in Chapter 3. The system consists of three main functional blocks namely surrounding information extraction, threat assessment, and response as shown in Fig. 2.1.

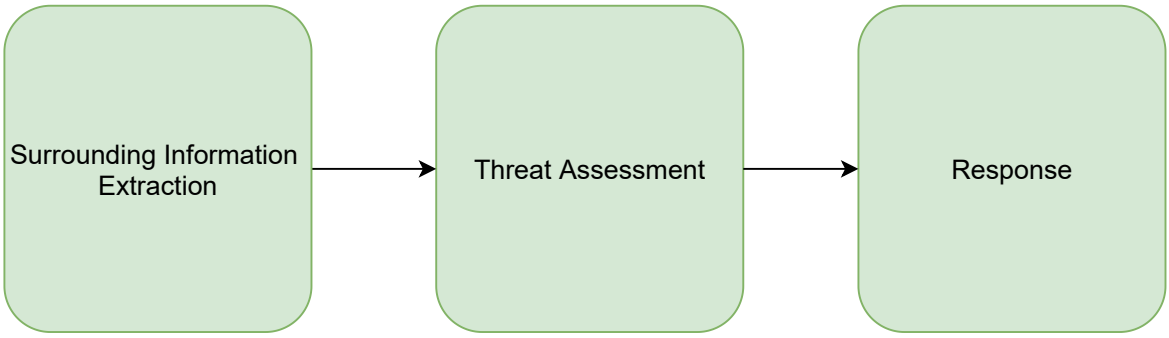

Figure 2.1: System Functional Blocks

2.1 Surrounding Information Extraction

This block is responsible for detecting other road users rapidly approaching from behind as well as present in close proximity around the host bicycle. The required information such as distance, position, and relative speed of desired detected targets such as bicycles, cars, and trucks need to be extracted for threat assessment. It has a direct impact on the overall performance of the system, as it acts as a bridge between the environment and the system. An error in the interpretation of the surroundings itself affects the accuracy of the assistance provided by the system significantly. The different sensing methods available for the implementation of this block are analyzed and evaluated in Section 3.1. The criteria that are considered critical for this block along with their requirements are as follows:

- **Range:** The range is defined as the maximum distance at which the sensor can detect targets. The increase in the range of the sensor enables the detection of distant vehicles in advance. The earlier the vehicles are detected more processing

time is available to process the information and deliver on-time warnings. Considering the speed of different vehicles on road, it was concluded that a minimum of 20m range is required for detecting closing vehicles in-order to provide warnings with minimum reaction time. However, the greater the range, the better.

- **External Sensitivity:** External Sensitivity is defined as the impact of external environmental factors on the performance of the sensor. The system requires a sensor with the least sensitivity that provides stable performance across adverse environmental conditions. This requirement is because the bicycle will be driven in all weather conditions and cyclists will depend more on the system during unfavorable environmental conditions such as fog, rain, etc. This reliance is caused by the reduction in the capacity of the cyclists to be aware of the surroundings under these difficult circumstances.

- **Estimation Capability:** Estimation capability is defined as the ability of the sensor to estimate characteristic features of the detected targets. This project requires a sensor that can estimate the speed, distance, and position of the detected targets. These features are considered vital for evaluating the safety of the lateral maneuver effectively.

- **Multi-Target Detectability:** Multi-target detectability is defined as the ability of the sensor to detect multiple targets in the scene. This capability is considered vital for the system as there will be multiple road users and each of them must be detected in order to evaluate the safety of the lateral maneuver effectively.

- **Field of View (FoV):** FoV is defined as the detection coverage of the sensor. This project requires a sensor with a considerable wide field of view as there is a need to monitor targets in the adjacent sides to determine the safety of the lateral maneuver. The increased FoV will enable the system to provide support for wider lateral maneuvers.

- **Accuracy:** Accuracy is defined as the ability of the sensor to detect targets correctly and estimate their characteristic features, as close to the original ground-truth value. This project requires a good accuracy rather than very high accuracy, as the system only assists the cyclists rather than executing the maneuver itself as in autonomous vehicles. The more accurate, the better.

- **Cost:** Cost is defined as the amount of money required to purchase the hardware components and build the system. This project requires a low cost sensor as it developed for a low-end vehicle. The increase in cost will restrict the feasibility of the system.

- **Complexity:** Complexity is defined as the amount of difficulty in implementing the sensor to detect targets and extract their characteristic features. This project requires a sensor with minimal complexity as the rise in complexity may result in higher hardware requirements, increased energy usage, mounting difficulty, and higher cost.

2.2 Threat Assessment

This block is responsible for evaluating the risk factor held by each detected road user from the information extraction block, to discover hazards that may impair the safety of the lateral maneuver. There are existing methods and algorithms to carry out this assessment and each of them have a performance level associated with them. Some of the most used methods and algorithms in existing systems are analyzed to find the challenges in implementing them for bicycles in Section 3.2. The criteria that are considered critical for the threat assessment block along with their requirements are as follows:

- **Complexity:** Complexity is defined as the amount of difficulty in obtaining the necessary information and implementing the assessment algorithm, to detect threats in the surrounding environment. This project requires an algorithm with minimal complexity as the rise in complexity may result in increased computation, energy usage, number of sensors for obtaining necessary information, and hardware requirements.

- **Accuracy:** Accuracy is defined as the ability of the algorithm to correctly estimate the threat possessed by the detected targets in the safe execution of the lateral maneuver. This project requires a relatively good accuracy as the system only assists the cyclist rather than very high accuracy, as in systems executing the maneuver itself.

- **Acceptability:** Acceptability is defined as the ability of the algorithm to estimate threats in a human-like manner to be acceptable by cyclists. This project requires a highly acceptable algorithm, as the utility of the system will only be obtained if the cyclists accept the system and make their decision based on the information provided.

2.3 Response

This block is ultimately responsible for providing the utility of the system to cyclists. It utilizes the position information of the threats assessed in the threat assessment block to provide timely assistance for cyclists during potentially dangerous maneuvers and enable safe maneuvers. The criteria that are considered critical for the response block along with their requirements are as follows:

- **Complexity:** Complexity is defined as the amount of difficulty in implementing the response mechanism to provide assistance to cyclists. This project requires a response mechanism with minimal complexity due to the restricted cost.

- **Utility:** The utility is defined as the usefulness of the assistance provided by the response block to improve cycling safety. This project requires a response mechanism that provides maximum utility based on the obtained information of the threats.

Chapter 3

State-of-the-Art and Critical Analysis

In this chapter, the available methods used in cars and bicycles for the implementation of each functional block are introduced. The methods used in cars are also studied due to the limited available systems implemented for bicycles and the feasibility of adapting methods used in cars is investigated. The feasibility of each method is analyzed using the criteria mentioned for each functional block as mentioned in Chapter 2.

3.1 Surrounding Information Extraction

There is a wide range of sensor technologies that are available for the extraction of surrounding information in ADAS. These technologies are broadly classified into three major categories vision-based, non-vision-based, and vehicular communication methods. They will be reviewed in this section.

3.1.1 Vision Based Sensors

This category includes sensors that capture the surrounding environment using different types of cameras and various image processing algorithms are then applied to detect road users and extract their information such as speed and distance. These sensors are versatile and are capable of producing higher-resolution information, as well as color and texture data, but their detection range is relatively low and is easily affected by poor weather conditions. The two main types of vision-based systems employed in road safety assistance systems are Monocular and Stereo systems.

1. **Monocular System:** These type of systems use a single camera sensor to capture the surrounding video. It is the popular system type used in on-board road safety systems and is capable of detecting vehicles, lane marks, traffic signs, and pedestrians reasonably well. The shortcoming of the system is its inability to calculate a robust and reliable 3-D view of the world from the planar 2-D frame that is received from the camera sensor.

2. **Stereo System:** These type of systems use two camera sensors separated from each other to capture the surrounding video. They provide a 3D image by combining the images from two cameras sensors, which results in easier obstacle detection.

The distance to the detected objects can also be measured accurately through triangulation. The shortcomings of these systems are their increased cost and complexity.

This technology has been widely used in cars with very limited work in bicycles. They have been mostly used in ADAS that aid in lane change detection and lane change decision on car [15] [19] [20] [21] and to monitor closing vehicles on bicycles [16]. They are seen to have high performance under certain ideal conditions with the capability to provide rich information of the surroundings for identification and classification requirements. But, require high-level indirect computation algorithms for the extraction of information such as speed and distance of vehicles which are crucial for ADAS that aid in lane change assistance or lateral maneuver to compute the safety of the maneuver effectively. They are also highly sensitive to illumination and weather conditions. Despite work to overcome these drawbacks through different image processing methods [20] [21], sufficient progress has not been made to match the performance of some non-vision-based technologies.

3.1.2 Non-Vision Based Sensors

This category includes sensors that capture the surrounding environment using different wave propagation-based sensing technologies. This category of sensors is growing in prominence with the advancements in wave propagation-based technologies. The key benefit of these technologies is their ability to immediately offer valuable information like speed and distance, making them simple to integrate into the road-safety assistance systems. Some of the common sensing technologies of this category that have been used in road-safety assistance systems are ultrasonic sensors, acoustic detectors, radars, and lidars. These methods will be explained and reviewed.

1. **Ultrasonic Sensor:** Ultrasonic sensors are one of the oldest sensor technologies that have been used in road-safety applications. They use reflected sound waves to calculate the distance to targets. The sensor transmits short bursts of ultrasonic sound waves and measures the time taken for the sound to travel to a target, be reflected, and return to the receiver as shown in Fig. 3.1. The distance to the object is estimated based on the travel time and the speed of sound in the air. Their detection range is limited to around 4m, due to their atmospheric attenuation properties. The speed of sound in air is also influenced by temperature, humidity, and wind which may affect its performance in extreme outdoor conditions. Overall they are a cost-effective, relatively robust, and reliable sensing technology for short-range detection. They have been used mostly in blind-spot warning systems for cars and bicycles [17] [22]. They are cost-effective and relatively robust, but their short sensing range and their inability to estimate the speed and position of vehicles have restricted their usage in ADAS with other complex functionalities.

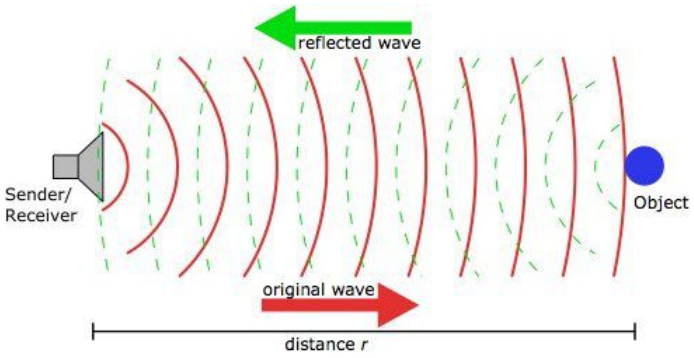

Figure 3.1: Ultrasonic Sensor Working [23]

2. **Acoustic Detector:** Acoustic detectors are passive sensor technology that has been used for vehicle detection. They use an array of microphones to capture the sound signals from the surrounding environment as shown in Fig. 3.2. These signals are then processed and correlated using machine learning algorithms to obtain information about the vehicle passage. The FoV and the directionality of the detector depends on the microphone array design. These types of sensors have been used in some road-safety applications. They have been used for closing vehicle detection in bicycles [18], but their performance has not been thoroughly investigated. The accuracy of the systems is seen to be high, but the range of detection and complex processing algorithms are a constraint. The ability of these sensors to detect road users such as bicycles and pedestrians that do not emit significant sound during their movement is still an open challenge that has not been addressed.

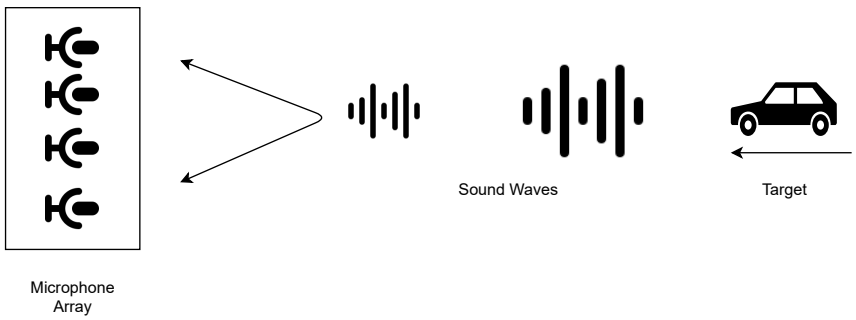

Figure 3.2: Acoustic Detector Working

3. **Radio Detection and Ranging (RADAR):** Radars are an electromagnetic-based sensor technology used for detecting, and recognizing targets at considerably long distances. They operate by transmitting electromagnetic waves toward objects and observe the echoes returned from them to determine their presence, location, and velocity as shown in Fig. 3.3. Their ability to detect faraway targets under adverse weather conditions and determine their range and distance with precision distinguishes them from optical and infrared sensing methods.

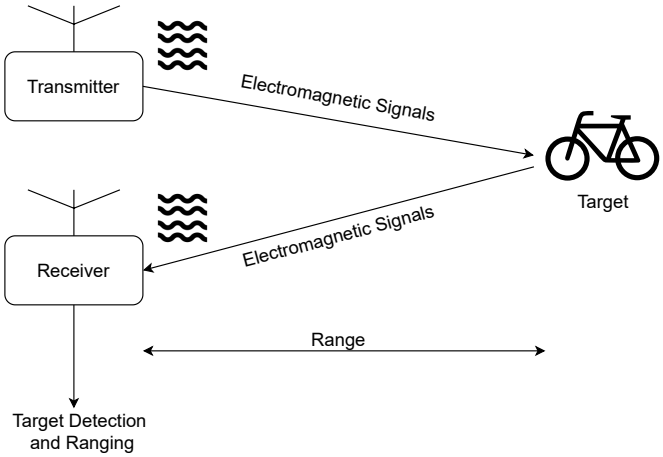

Figure 3.3: Radar Sensor Working

Radars are broadly classified based on the frequency of their operation as shown in Fig. 3.4. Each frequency band has its own performance capabilities. The factors such as physical size, transmitted power, antenna beamwidth, and atmospheric attenuation vary with frequency.

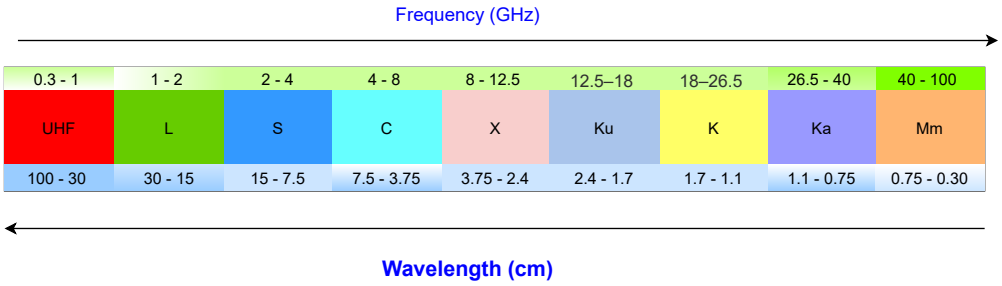

Figure 3.4: Radar Operation Bands

Physical Size: The size of the radar hardware is directly proportional to the wavelength of each band. The wavelengths are shorter for higher frequency bands, resulting in small hardware that can be housed in smaller packages.

Transmitted Power: The ability to transmit larger amounts of power is indirectly dependent on the wavelength of the band due to its impact on the hardware size. Thus, larger the wavelength, higher the transmitted power.

Beamwidth: The ratio of the wavelength to the width of the antenna determines the width of the radar's antenna beam. To create acceptable narrow beams at low frequencies, huge antennas are usually required. Small antennas will suffice at higher frequencies.

Atmospheric Attenuation: The atmospheric attenuation increases with frequency. It is negligible up to 100 MHz, above which it becomes increasingly important.

The millimeter (Mm) band uses the shortest wavelength among the electromagnetic waves that are in the millimeter range. These short wavelengths are considered to be one of the major advantages, as it results in smaller system components such as antennas and higher detection accuracy. The radars that operate in this band are

known as mmWave radar. The modern mmWave radars exhibit distinct advantages over lower band (L, C, X, Ku, K, Ka) radars such as:

- Lower Radar Cross Section (RCS).
- Longer detection range.
- Enhanced spatial resolution.
- Agile maneuverability.
- Superior survivability.
- All weather capabilities and greater reliability.
- Increased accuracy.
- Reduced size, weight, power and cost.

Radars have been increasingly used in automotive and industrial applications over the last decade. The 24GHz frequency band has been used in legacy radars that are widely implemented in cars with very limited implementation in bicycles. They have been implemented in applications such as forward collision warning, blind-spot warning, autonomous emergency braking, and adaptive cruise control in cars [24] [25] [26] [27] [28]. Their implementation on bicycles for closing vehicle warning and forward obstacle detection systems are in development stages [29] [30]. This band has a few shortcomings with respect to power, size, and accuracy as mentioned above. But, the spectrum regulation and standards developed by the European Telecommunications Standards Institute (ETSI) and Federal Communications Commission (FCC) has mainly lead to the shift towards the higher 77GHz-81GHz band (mmWave). The mmWave radars are emerging as a key technology in cars with increased implementation, but there has been no known implementation in bicycles. They have been used in ADAS that provide automatic emergency braking, blind-spot detection, pre-collision warning, automatic cruise control, pedestrian identification, and autonomous driving [31] [32] [33] [34] [35]. Angular resolution and target classification capabilities are mainly known to be their current limitations.

4. **Light Detection and Ranging (LIDAR):** Lidars essentially work on the same principle as radar but swap electromagnetic waves for lasers. They operate by projecting an optical pulse at a target and analyzing the properties of the reflected return signal as shown in Fig. 3.5. They can detect faraway objects similar to radars but have difficulty detecting close objects. They are capable of providing an extremely high-resolution 3D characterization of targets without significant back-end processing and their high spatial resolution in the order of 0.1 degrees differentiates them from radars. Their performance is affected by ambient light conditions and degrades in adverse weather conditions. They are also seen to be increasingly gaining their way into ADAS systems in cars with very minimal usage in bicycles. They are used in collision warning and avoidance systems, blind-spot monitors, lane-keeping assistance, adaptive cruise control and focused towards autonomous driving in cars [36] [37] [38] [39] [40]. They have been used for front obstacle detection and avoidance in bicycles [41]. Their performance is similar to radars apart from the improved spatial resolution. But their high cost and sensitivity to adverse weather conditions have limited their usage.

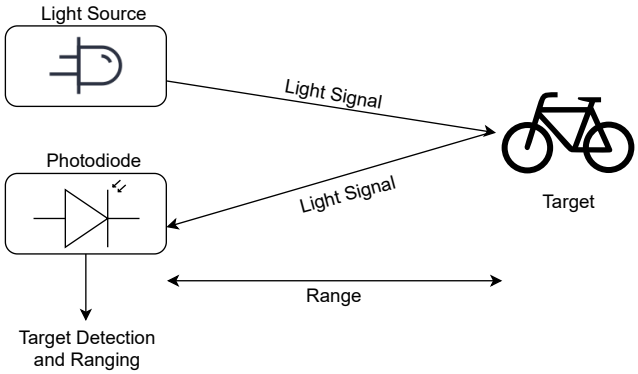

Figure 3.5: Lidar Sensor Working

3.1.3 Vehicular Communication

Vehicular communication is one the emerging research field and can be viewed as the new generation of automotive sensor technology for road-safety applications. They felicitate the exchange of information between the vehicles and surrounding environment as shown in Fig. 3.6 and enable to design the next generation of ADAS. The communication network includes Vehicle-to-Vehicle (V2V), Vehicle-to-Road Infrastructure (V2I), and Vehicle-to-Pedestrians, where the road infrastructure and the users are equipped with wireless communication devices and exchange information between them. These interactions enhance the situational awareness of vehicles and provide drivers with an information-rich travel environment. Further, connected vehicles are considered as the building blocks of the emerging Internet of Vehicles, a dynamic mobile communication system that features gathering, sharing, processing, computing, and secure release of information and enables the evolution to next generation Intelligent Transportation Systems [42]. The development and deployment of fully connected vehicles requires a combination of various off-the-shelf and emerging technologies, and great uncertainty remains as to the feasibility of each technology. Thus, there are still a lot of uncertainties and challenges to be addressed for the deployment of connected vehicles on a large scale. There is extensive research on V2V and V2I communication networks [43], with researchers also attempting to include bicycles into the network using Bicycle-to-Vehicle (B2V) and Vehicle-to-Bicycle (V2B) communication systems [44]. Lane change assistance systems have also been implemented using this technology in cars [45] [46]. The researches in this domain only aim to develop basic system framework and test its performance under limited test scenarios. Implementation of these systems at scale require a new infrastructure which will be expensive and time consuming.

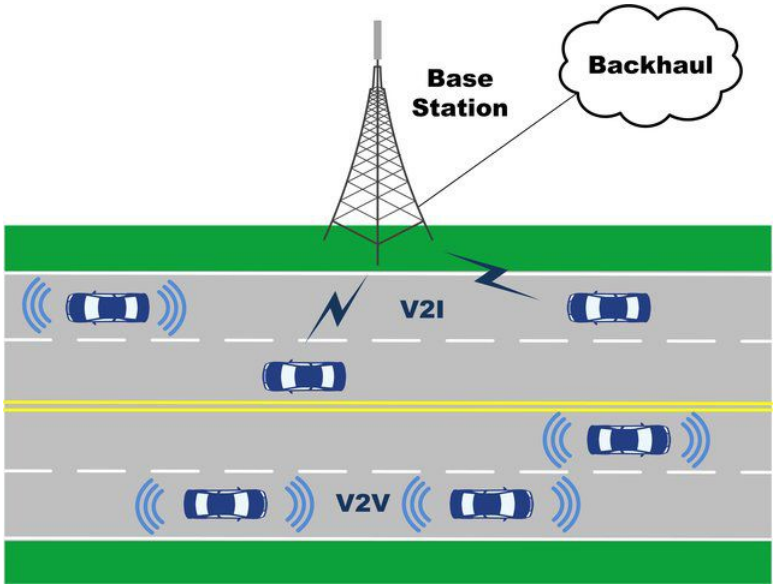

Figure 3.6: Vehicular Communication Working [47]

3.1.4 Sensor Fusion

Sensor fusion is the method of bringing together inputs from multiple sensors such as radar, lidar and camera to improve the accuracy of resulting information by balancing the strengths of different sensors. It enables to provide the most comprehensive, and therefore accurate, surrounding environmental model possible. Most of the existing ADAS adapt sensor fusion to achieve high level accuracy of object identification and tracking to meet the requirements of autonomous driving. This method is mostly implemented in cars [7] [48] [49] [50] [51] [52], with limited adaptation in bicycles [53]. Almost all the existing fusion methods have resulted in the increased system complexity and cost as only high performance sensors such as lidar, camera, and radar are used together.

3.1.5 Comparison of SoA methods

The selection of suitable sensor technology for obtaining the surrounding vehicle information is one of the important design decision that needs to be taken. The vision based methods are popularly used in LCDAS with significant work also being done using vehicular commu-nication in cars. The popularity of vision based sensors are inferred to be mainly due to their capability to identify the lane separation markings on the road, which is not the case in bicycles. We assume a approximate common lateral displacement of the maneuver, as there are no clear lane separation in most scenarios. The vehicular communication method is still evolving and will assure safety only in an infrastructure, where other bicycles and vehicles are also equipped with the same system, which is not the case in the current scenario. Thus, the methods of these two categories are concluded not be suitable for the project due to their increased cost, computational complexity, sensitivity to adverse weather conditions, and futureness. The existing fusion methods are also concluded not be suitable for the project due to their cost and complexity. The non-vision based methods are the only remaining category and concluded to be most suitable for the project, mainly due to their ability to provide useful information such as speed and distance of targets without the need of complex algorithms. There are several

sensor methods in this category and each method is inferred to have its own benefits. The best suited technology for this project, from this category is selected by comparing the methods based on the criteria that were identified to be the crucial for project in Section 2.1.

	Ultrasonic	Acoustic	24GHz Radar	mmWave Radar	Lidar
Range	<4m	<10m	<150m	>200m	>200m
External Sensitivity	High	High	Low	Low	High
Estimation Capability	Distance	Distance	Distance, Speed, Angle	Distance, Speed, and Angle	Distance, Speed, Angle
Multi-target Detectability	No	No	Yes	Yes	Yes
FoV	Less than 15°	-	Up to 120°	Up to 120°	Up to 360°
Accuracy	Moderate	High	High	Very High	Very High
Complexity	Very low	High	Moderate	Moderate	Moderate
Cost	Very low	Low	Moderate	Low	Very High

Table 3.1: Non-Vision Based Information Extraction SoA Methods Comparison

The Table 3.1 shows the comparison of the methods, and it is evident that lidar and mmWave radar are the methods that align the most with the requirements. The major difference between these methods is the ability of the lidar to provide an enhanced coverage to detect targets in the rear-side blind-spot regions as well as approaching from the rear. But its increased external sensitivity and cost are the major shortcomings. The mmWave radar method has been gaining popularity in cars, but its benefits are yet to be explored in bicycles. The only drawback of this method is the restricted FoV, which limits the detection of targets on the rear-side blind-spot regions.

3.2 Threat Assessment Methods

The threat assessment methods allow to estimate the risk of collision possessed by a target with the host bicycle, that enable to evaluate the safety of the lateral maneuver. The deterministic and probabilistic approaches are the two most popular methods of threat assessment.

3.2.1 Deterministic Method

The deterministic method offer a binary prediction, that only estimate whether a potential collision will happen or not. It is a rule-based method that computes the output prediction by comparing a conservative estimate of prospective exposure to the threshold risk value. It is simple and computationally efficient and has been deployed in various collision mitigation systems. One of the drawback of this approach is the inability to explicitly

model the uncertainties of its input data. The common metrics used to estimate the risk of a collision as a binary prediction are as follows:

- **TTC:** It is the most well-known time-based safety indication. It represents the time until a collision between two objects occurs. The most frequently used computation formula is the relative distance to the target object divided by the relative velocity [54].
- **Time-to-Brake (TTB):** It is also a time-based safety indicator that is derived from the TTC metric. TTB denotes the remaining time until an emergency braking at maximum deceleration must be applied to avoid the collision by braking [55].
- **Time-Headway (THW):** It is a measure of the temporal space between two vehicles. It is defined as the inter-arrival time difference between the leading vehicle and the following vehicle at a designated test point on a traffic lane [56].
- **Deceleration-to-Safety-Time (DST):** It is a safety indication that is dependent on acceleration. It calculates the amount of deceleration necessary for a vehicle to achieve a non-negative gap time when compared to another road user [57].
- **MSD:** It is a distance-based safety indicator. It is defined as the minimum distance to be kept between the host and the obstacle [54]. This metric is aimed for situations where spatial margins are important.

This approach has not been widely used for assessing threats in a lane change assistance ADAS. Only one research was found to use this method for providing adaptive cruise control with lane change assistance in cars [10]. The negligence of the speed of the surrounding vehicles and the vehicles in the blind spots parallel to the host vehicle is one of the major shortcomings of the algorithm that restricts its performance. This approach is simple and computationally efficient, its inability to explicitly model the uncertainties of its input data is one of the major shortcomings.

3.2.2 Probabilistic Method

The probabilistic method utilizes a probabilistic description to model the risk level by using the temporal and spatial relationships between vehicles. The risk is defined using the severity of the potential negative outcomes and the likelihood of each consequence occurring. It also incorporates the uncertainties of input data into the threat assessment. The most common models used in this method are as follows:.

- **Bayesian Networks:** It is a probabilistic graphical model that represents a set of variables and their conditional dependencies via a Directed Acyclic Graph.
- **Fuzzy Logic:** It is a new mathematical tool to model inaccuracy and uncertainty of the real world and human thinking. It is computed based on the "degrees of truth" rather than the standard Boolean logic used by the modern day computers [58].
- **Markov Processes:** It is a process that involves the prediction of the likelihood of a future action, given the current state of a variable. The likelihood of a result is determined by drawing a decision tree based on the determined probabilities of future actions at each state.

This approach is increasingly becoming the standard for threat assessment in lane change assistance systems in cars and are mostly focused towards autonomous vehicles [11] [12] [13] [14]. It is a comprehensive approach that enables to make more informed decisions and adapt appropriate strategies for different scenarios. It also incorporates input data uncertainties into a threat assessment uncertainties of input data. The disadvantage of this approach is its computing complexity, which stems from the large number of input elements to consider.

3.2.3 Comparison of SoA Methods

An assessment algorithm is required to calculate and compute the safety of a maneuver based on the surrounding information obtained from the information extraction block. The concentration of existing lane change assistance systems on cars, has resulted in complicated probabilistic approach based assessment algorithms geared towards autonomous driving. They are not suitable for the project due to their complexity and superfluous performance. Some of the few systems that adapt deterministic approach based algorithms are use metrics only based on the spatial relationships between vehicles. They are simple but not acceptable enough, with a lot of scope for performance improvement. The common threat assessment metrics available for deterministic based approach are compared based on the requirements mentioned in Section 2.2.

Criteria	TTC	TTB	THW	DST	MSD
Complexity	Low	High	Moderate	High	Low
Acceptability	High	Low	Moderate	Low	Moderate

Table 3.2: Deterministic Approach Metrics Comparison

The Table 3.2 shows the comparison of the commonly available metrics. The TTB and DST are similar time based metrics that are inferred to be highly complex due to their additional parameter consideration such as acceleration and braking capacity apart from distance and speed. These additional information are not readily available and require additional sensing hardware. They are also more correlated to avoid forward collisions, as it not practically possible to obtain the required additional data of the targets. The THW metric has a relatively better acceptability at lower complexity, but it only takes the speed of the approaching vehicle, which is also a challenge to obtain using the available methods of the information extraction block. Thus, these metrics are deemed not to be suitable for the project. The remaining two metric MSD and TTC are inferred to align the most for the current project. The MSD is a distance based metric, and gives the minimum spatial distance that must be maintained around the host bicycle. It is used to provide minimal reaction time to the following vehicle in the case of speed reduction of the leading vehicle, in-order to avoid collision and can also be used to detect obstacles within the lateral displacement of the maneuver on the sides. The TTC metric physically presents the difference in speed and spatial proximity and was inferred that the decision of drivers to perform the lane change maneuver which also incorporates lateral maneuver, is highly correlated to this metric [59]. The major shortcoming of this metric is its inability to cover situations, where an observed vehicle is at close proximity to the host bicycle and is travelling at a similar speed. In this situation, the value of the TTC will be much higher and the situation will be assessed as low risk. However, a lateral maneuver under this situation will be dangerous and the maneuver must not performed.

3.3 Response

This block can have two types of implementation based on the type of the assistance system. The two types of system are warning type and intervening type.

3.3.1 Intervening Type

These systems directly intervene in the actual movement of the vehicle by taking over vehicle control from the driver during certain tasks. This type of lane change assistance system perform the maneuver task end to end. The system collects the surrounding information, plans the change trajectory and follows the planned trajectory to complete the maneuver. They are more complex and require powerful hardware to implement the control mechanism in real-time.

3.3.2 Warning Type

These systems warn the driver/cyclist of any potential danger via the optical, acoustic, or tactile sensory channels of human beings. These warning systems focus more on providing supporting information to the driver/cyclist to enable better control decision making for safer maneuvers. The responsibility still lies with the driver/cyclist for making use of the information to improve the overall safety. The advantage of warning type is their reduced complexity of implementation.

3.3.3 Comparison of SoA Methods

This block is ultimately responsible for providing the utility of the assistance system to the driver. The intervening type implementation is seen to be more popular in lane change assistance systems on cars [10] [11] [12] [13]. These systems directly intervene in the actual movement of the vehicle by taking over control, they collect the surrounding information, plan the change trajectory and follow the planned trajectory to complete the maneuver. There are also a few systems that have a warning type implementation [20] [21]. These systems focus more on providing supporting information to the driver to enable better control decision making for safer maneuvers. The warning type implementation is suitable for current project due to the unstable vehicle dynamics of bicycles, where active intervention may be dangerous for cyclists. The challenge of this implementation is to decide on the information that is conveyed to cyclist in order to be useful and acceptable, and the mode of communication of the information to the cyclist.

3.4 Summary

- Vision-based sensors have been widely used for LCDAS in cars, mainly due to their capability to identify the lane separation markings on the road, which is not the case for bicycle road infrastructure.
- Most of the existing ADAS solutions that adapt sensor fusion are expensive and complex, as they aim to achieve very high level accuracy of object identification and tracking to meet the requirements of autonomous driving.

- The sensors used by existing ADAS in bicycles suffer from drawbacks such as sensitivity to weather, reduced detection range, and minimal information estimation capabilities.
- The mmWave radar method has been gaining popularity in cars, but its benefits are yet to be explored in bicycles. The restricted FoV, that limits the detection of targets on the rear-side blind-spot regions is their major shortcoming.
- The threat assessment algorithms used in existing lane change assistance systems are either only based on the spatial relationships between vehicles and, do not provide sufficient performance to be acceptable by the user or are too complex and focused towards autonomous vehicles.
- Intervening type implementation is seem to be common among existing lane change assistance system in cars and is deemed unsuitable for bicycles, as their balance for optimal motion is entirely dependent on the cyclist, due to their vehicle dynamics. Active intervention may results to be dangerous for cyclists.

Chapter 4

Theory and Background

In this chapter, a general introduction to understand the functioning of the mmWave FMCW radar used in the project is provided. This information will help to understand the radar configuration trade-off mentioned in Section 5.2.1.

4.1 Fundamentals of FMCW Radar

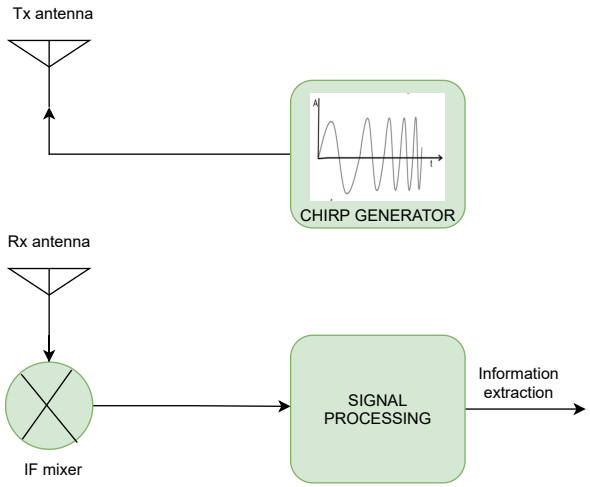

Figure 4.1: FMCW Radar Working

The Fig. 4.1 shows the basic working principle of a mmWave FMCW radar, that is used in the project. It transmits a sinusoidal signal whose frequency increases linearly with time (chirp) through the Transmitter (TX) antenna and the chirp reflected by a target is received through the Receiver (RX) antenna, and mixed with the transmitted chirp. The mixer combines these two signals and produces an output signal known as the Intermediate Frequency (IF) signal, which has an instantaneous frequency and phase equal to the difference of the two input chirp signals according to Eq. (4.1), where x_{out} is the output IF signal, w_1 and w_2 are the frequencies of the input signals, and ϕ_1 and ϕ_2 are the phase of the input signals. This IF signal is further processed to obtain the range, velocity, and angle information of the target.

$$x_{out} = sin[(w_1 - w_2)t + (\phi_1 - \phi_2)] \tag{4.1}$$

4.2 Range Estimation

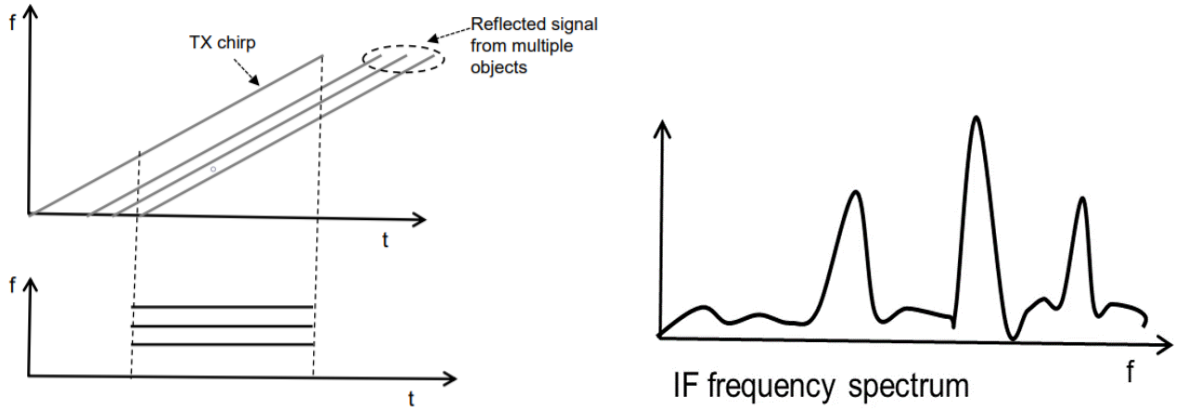

(a) Time Domain (b) Frequency Domain

Figure 4.2: Range Estimation Principle [60]

The chirps reflected by objects are the time delayed versions of the TX chirp that can be expressed as in Eq. (4.2), where τ is the time delay, d is the distance of the reflected target, and c is the speed of light. The IF signal consists of multiple tones, respective to each object and is given by Eq. (4.3), where S is the slope of the chirp. The Fast Fourier Transform (FFT) processing of this IF signal, results in frequency spectrum with peaks corresponding to different tones that are proportional to the range of a target. This process can be seen in Fig. 4.2. The ability of two reflections to show up as separate peaks is known as the range resolution, and depends on the chirp bandwidth according to Eq. (4.4), where d_{res} is the range resolution, c is the speed of light, and B is the bandwidth of the chirp.

$$\tau = \frac{2d}{c} \tag{4.2}$$

$$f_{IF} = S\tau \tag{4.3}$$

$$d_{\text{res}} = \frac{c}{2B} \tag{4.4}$$

4.3 Velocity Estimation

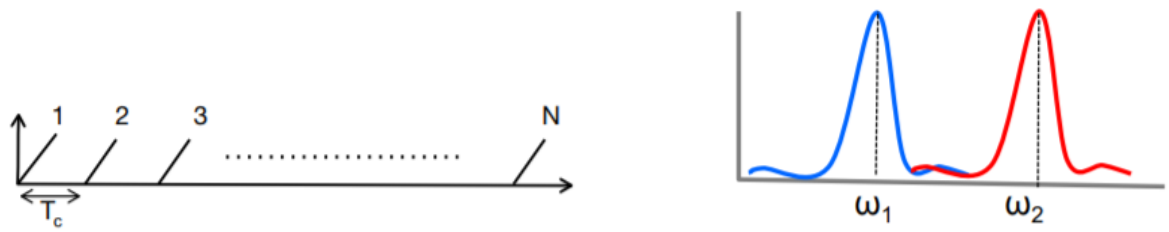

(a) Radar Frame

(b) Doppler FFT

Figure 4.3: Velocity Estimation Principle

A minimum of two chirps separated by a time interval Tc are required for the velocity estimation of targets. The signals in the frequency domain are in complex form with amplitude and phase. The range FFT of each reflected chirp results in a peak on the same location but with different phase. This phase difference is due to the motion of the target and its relation is given by Eq. (4.5), where v is the velocity of the target, λ is the wavelength of the chirp, and $\Delta\phi$ is the phase difference between the two chirps. The phase of the IF signal is highly sensitive to very small range difference in the factor of 1 millimeter. However, two chirps would not be enough to estimate the velocity of two objects at the same distance from the radar and travelling at different velocities. The range FFT in this case will result in a single peak, which is the combined signal of both the targets. Thus, to overcome this the radar transmits a frame with N number of chirps. The range FFT of the RX chirps in the frame result in N identical peaks with different phase corresponding to both the targets. The second-FFT known as Doppler FFT is performed on these N chirps to resolve them as separate targets and their respective phase difference is used to estimate their velocity using Eq. (4.5). The ability of two difference velocities to be resolved as two peaks in Doppler FFT is known as the velocity resolution. It enables to resolve targets that were not resolved separately in range direction. It is given by Eq. (4.6), where T_f is the total frame time and is given by Eq. (4.7). The velocity measurement denotes the absolute velocity of the targets only when the radar is stationary. When the radar is mobile, the velocity measurement denotes the relative velocity of the targets with respect to the radar.

$$v = \frac{\lambda \Delta\phi}{4\pi T_c} \tag{4.5}$$

$$v = \frac{\lambda}{2\pi T_f} \tag{4.6}$$

$$T_f = NT_c \tag{4.7}$$

4.4 Angle Estimation

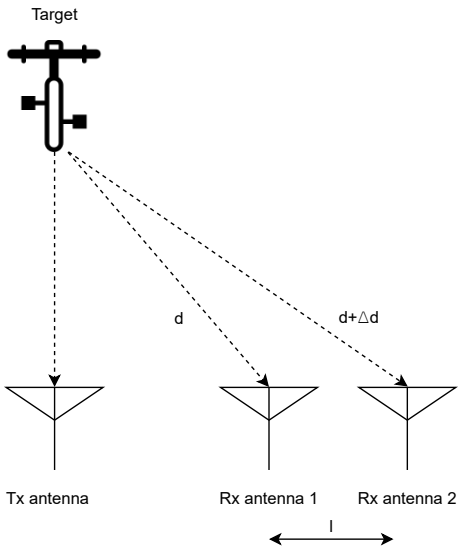

Figure 4.4: Angle Estimation Principle

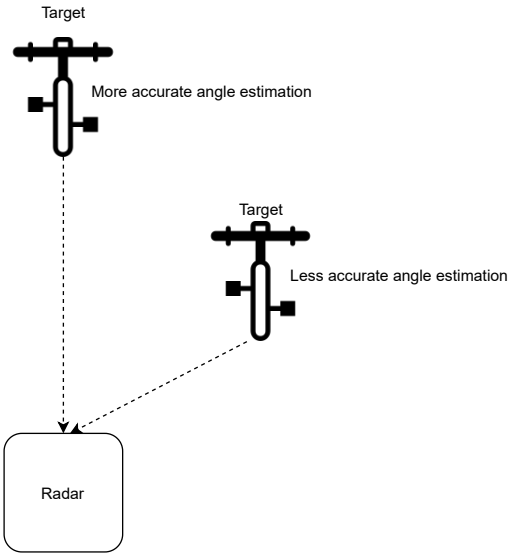

Figure 4.5: Angle Estimation Accuracy

The angle information of the targets denote the positional angle of targets with respect to the horizontal plane. This is an important information apart from range, that enables the localisation of the targets with respect to the radar. It is estimated using the similar principle used for velocity estimation and is based on the phase difference of the RX chirps. The only key difference is that the phase change across chirps separated in space are used for angle estimation, whereas chirps separated in time are used for velocity estimation. The RX chirps are separated in space by placing the RX antennas apart and a minimum of two RX antennas are required for angle estimation as shown in Fig. 4.4. The high sensitivity of the reflected signal phase to small range, requires only a very small distance between RX antennas. The phase difference $\Delta\phi$ between the chirps received in each RX antenna are used to estimate the angle of the target θ according to Eq. (4.8), where l is the distance between the antennas. The angle estimation accuracy is higher when θ is small and decreases as θ approaches 90° as shown in Fig. 4.5 due to the non-linear dependency of $sin\theta$ for larger θ values. The angular resolution of the radar depends on the number of receiving antennas N_{rx} according to Eq. (4.9). The maximum angular FoV depends on the spacing between the RX antennas according to Eq. (4.10).

$$\theta = \sin^{-1}\left(\frac{\lambda\Delta\phi}{2\pi l}\right) \tag{4.8}$$

$$\theta_{res} = \frac{2}{N_{rx}} \tag{4.9}$$

$$\theta_{max} = \sin^{-1}\left(\frac{\lambda}{2l}\right) \tag{4.10}$$

Chapter 5

Proposed Early Warning System For Safe Lateral Maneuver of Bicycles

In this chapter, a general introduction to understand the functioning of the early warning system for safe lateral maneuver of bicycles, developed in this project is provided.

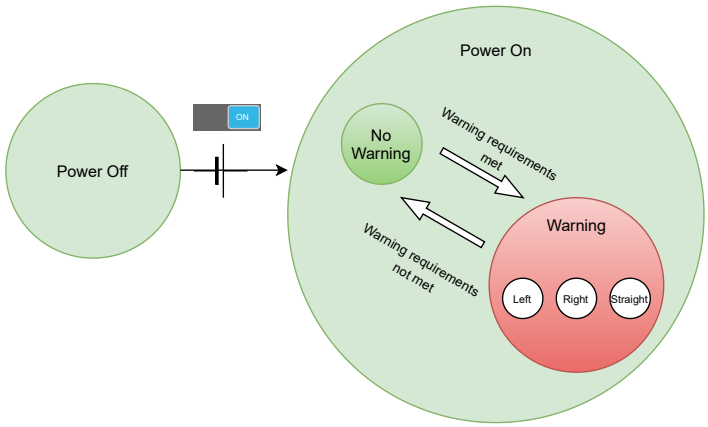

Figure 5.1: System State Diagram

The state diagram of the system is shown in Fig. 5.1. The system is initially in power off state and switches to power on state or ready state when power supply is provided. In ready state, the system continuously detects targets in the rear-side blind-spot regions and the targets approaching rapidly from behind. The violation of safety conditions by the detected targets is checked twice every second. If targets that violate these conditions are detected, then the system transits to the warning state, else it will be in no warning state. The warning state has sub-states based on the direction of the potentially dangerous maneuver.

5.1 System Overview

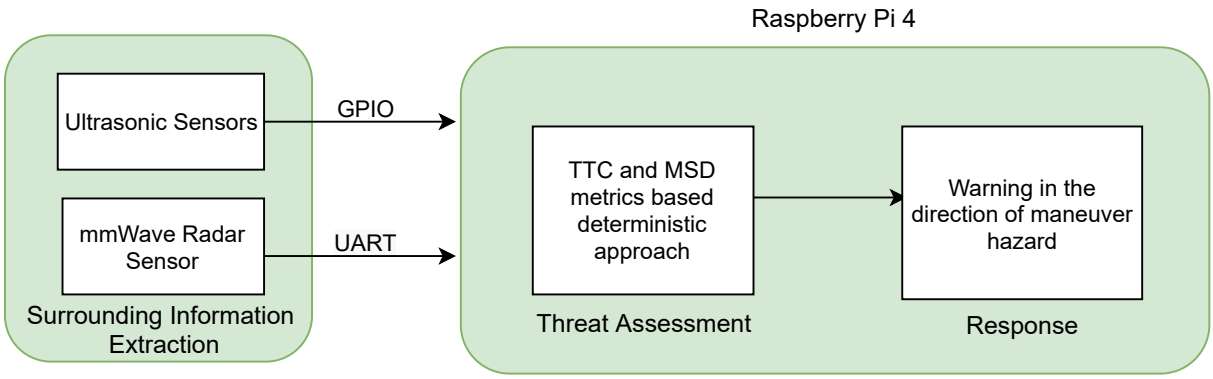

Figure 5.2: System Overview

The composition of the three main functional blocks of the system is shown in Fig. 5.2. The information extraction block is capable of detecting the distance of road users present in the rear-blind spot regions present close to the rear wheel of the bicycle users as well as position, and velocity of targets approaching from behind using the sensor combination of ultrasonic and mmWave radar sensors. This combination complements their drawbacks with increased sensing coverage and enables stable detection across various weather and road conditions at reduced cost and complexity. The threat assessment block is implemented as a function in the Raspberry pi. It discovers hazards that may impair the safety of the lateral maneuver, using an improved deterministic based algorithm that evaluates safety in a human-like manner utilising the TTC and MSD metrics. It is much simpler and effective by also taking the speed metric into consideration. The algorithm evaluates safety in a human-like manner in order to reduce false positives and also be acceptable by the users. Its complexity is also kept to minimum in order to provide on-time alerts with less computing power and software. The response block utilises the position information of the threats assessed in the previous block and generates a timely warning of a potentially dangerous maneuver based on the direction. It also contains information to alert the driver of a dangerously approaching target right behind the host bicycle to avoid collision. This algorithm is implemented as a function in Raspberry pi. The warning information can be delivered to rider through a variety of means such as optical, acoustic, or tactile sensory channels of human beings. Haptic sensors on the handle bars of the bicycle is inferred as an ideal option, but it is not implemented in this project. The scope is restricted only till generation of useful warning information and evaluating its performance with an easy interface option to extend it through any communication means via the General Purpose Input Output (GPIO) pins of the Raspberry pi controller.

5.1.1 Hardware Overview

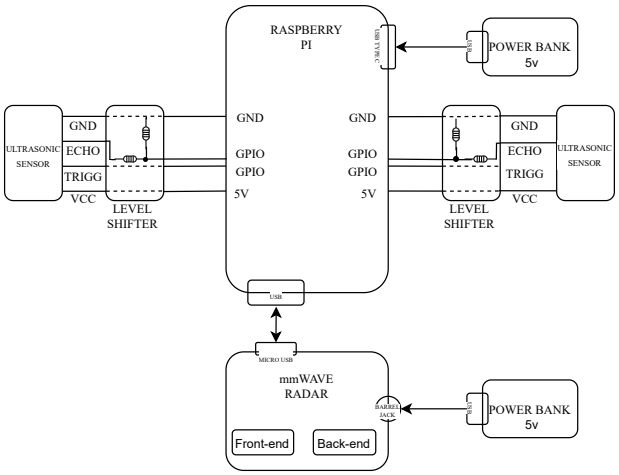

Figure 5.3: Hardware Implementation Block Diagram

The overall representation of the hardware components used for the implementation of all the functional blocks of the system with their interconnections is shown in Fig. 5.3. The mmWave radar sensor and two ultrasonic sensors used for the implementation of the information extraction block are connected to the Raspberry pi4 controller via USB-Universal Asynchronous Receiver Transmitter (UART) interface and GPIO pins respectively. A voltage divider circuit is used as an level shifter to bridge the GPIO connections between the ultrasonic sensors and the Raspberry pi 4 controller. This is necessary as the GPIO pins of the Raspberry pi only tolerate a voltage of 3.3v and the high level output of the ultrasonic sensors are 5v. The Raspberry pi4 is a low cost mobile computer with several peripherals for easy interface and is used as the main controller of the system. The threat assessment and the response block of the system are implemented on this controller. The computation capability of this controller is much higher than the system requirement, but is used to enable easier integration of further system functionalities in the future. It also has in-built Bluetooth and WiFi communication interfaces that can also be used to extend for Bicycle to Everything (B2X) applications. The system was powered using two mobile 5v powerbanks, one to power the Raspberry pi controller and the other to power the radar module. The system is inferred to consume only a minimal amount of power, as the single charge of a powerbanks lasted for multiple days of testing with 2 to 4 hours usage per day.

5.1.2 Software Overview

The software implementation of the system on the Raspberry pi controller is done using the python language and its flow is given in Fig. 5.4. The functions are implemented as individual threads, and queues are used for communicating between them. The main threads responsible for the functionality of the system are ultrasonic thread, radar thread, and the warning thread. The serial read and serial write threads are used as sub-threads for the functioning of the radar thread.

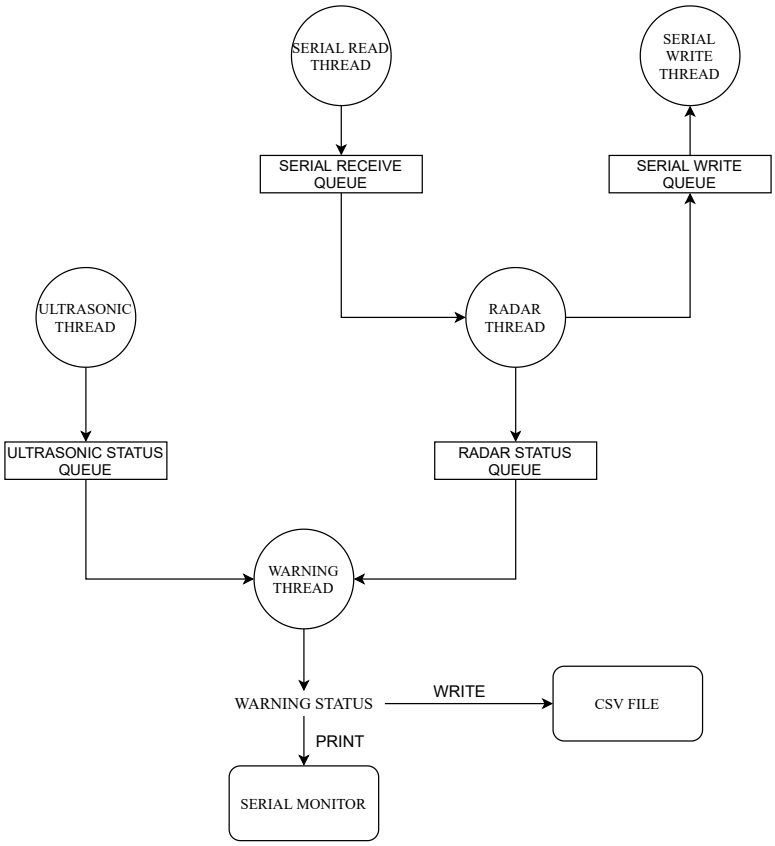

Figure 5.4: Software Flow Chart

- **Serial Write Thread:** This thread is responsible for sending out control instructions via the UART interface to the radar module. It is used to send the start command to the radar module on system bootup.

- **Serial Read Thread:** This thread is responsible for receiving the output frames from the radar module. It is used to listen to the UART port and store the received radar frame in the serial receive queue. This queue length is kept to one, to ensure that the latest frame is always made available for the radar thread.

- **Radar Thread:** This thread is responsible for parsing the latest frame received from the radar and determining the side and straight warning status information. The output of the evaluation is stored to the radar status queue in tuple form. The length of the radar status queue is kept to one, to ensure that the latest radar status is always made available for the warning thread.

- **Ultrasonic Thread:** This thread is responsible for controlling both the ultrasonic sensors, obtaining their respective detection information, and determining their warning information. The output of the evaluation is stored to the ultrasonic status queue as a single digit number. The length of the ultrasonic status queue is kept to one, to ensure that the latest ultrasonic status is always made available for the warning thread.

- **Warning Thread:** This thread is responsible for obtaining the warning status information from the radar and ultrasonic status queue to determine the warning status information of the overall system. The output of the evaluation is in tuple form and is printed on the serial monitor and also stored in a csv file with the timestamp. The serial monitor was viewed via a mobile phone with remote connection to the Raspberry pi while testing, and the csv file was used for ground truth verification.

5.2 Functional Blocks Realization

In this section, the design specifications and procedures carried out in this work for the implementation of each functional block are described in detail.

5.2.1 Surrounding Vehicle Information Extraction

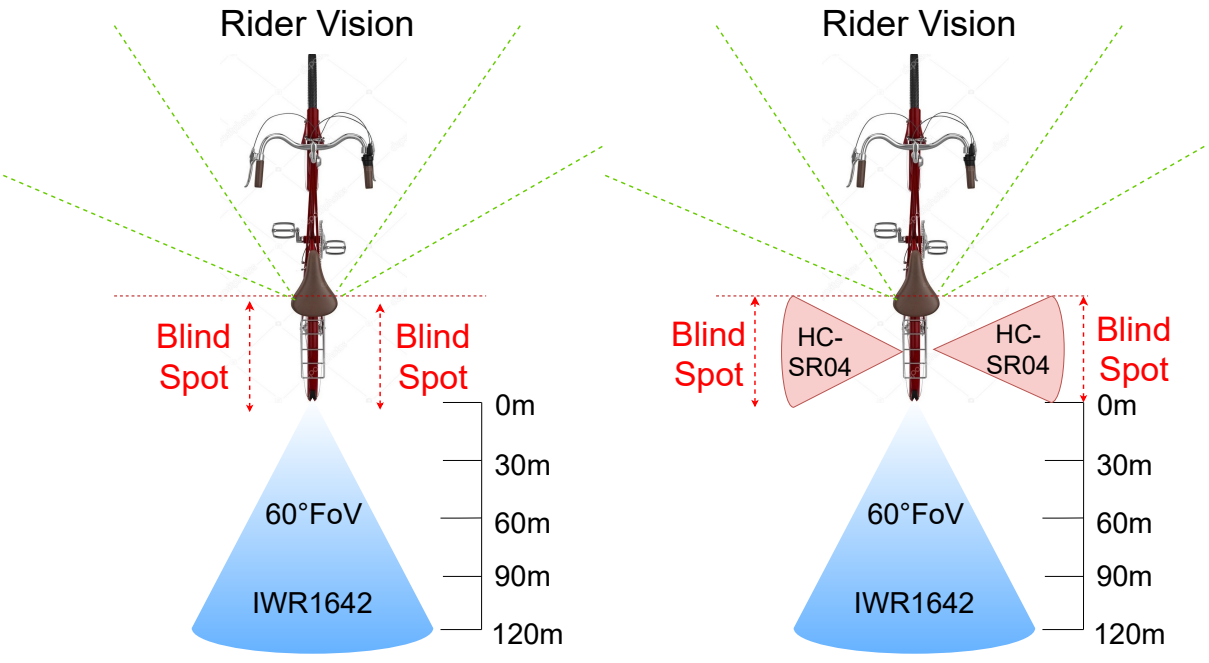

(a) No Ultrasonic (b) With Ultrasonic

Figure 5.5: System sensor coverage

The IWR1642 mmWave radar sensor from Texas Instruments and two HC- SR04 ultrasonic ranging modules are used for the implementation of this block. The integration of these sensors is inferred to improve the performance of the system by improving the sensing coverage and complementing their drawbacks, without increasing the cost and complexity. The region behind the cyclist is only assumed to be the coverage requirement of the system and the region in front is inferred to be the responsibility of the cyclist. This separation is based on the fact that it is easier for cyclists to monitor the surroundings in front, without major difficulty than in the rear. The Fig. 5.5a shows the coverage of the system only with the mmWave radar in the rear. It can be seen that the coverage

is limited to the rear and introduces the inability to monitor blind-spot regions close to the rear wheel of the bicycle on either side, that is also out of the coverage area the cyclist due to the restricted FoV of cyclist vision. The inability of the system to be aware of obstacles present in this region will affect the system performance in assessing the safety of the lateral maneuver significantly, as a vehicle or obstacle in these regions within close proximity of the bicycle will restrict the maneuver. Thus, ultrasonic sensors are integrated on either sides in the rear to extend the system detection coverage and improve the system performance as shown in Fig. 5.5b. Ultrasonic sensors are inferred to be the ideal low cost solution to improve the system coverage, as only close by targets need to be detected on the sides considering the width of the possible lateral maneuvers in real-road scenarios. The distance information of the obstacles in this region was inferred to be sufficient for threat assessment. This inference was based on the fact that the presence of an obstacle, within the displacement width of the lateral maneuver alone restricts the maneuver.

HC-SR04 Configuration and Processing

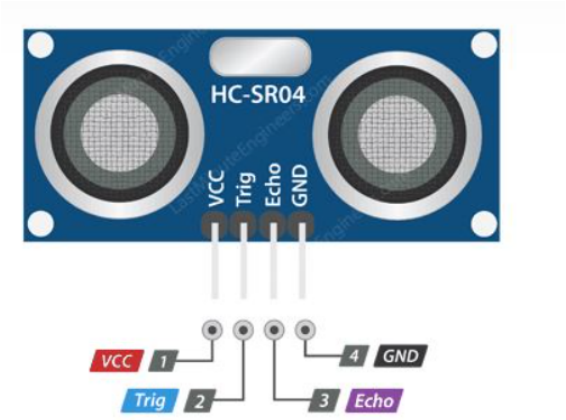

Figure 5.6: HC-SR04 Ultrasonic Sensor [61]

The HC-SR04 sensor consists of two ultrasonic transmitters, a receiver, and a control circuit and is shown in Fig. 5.6. Ultrasonic sound pulses at 40KHz are transmitted by the transmitters and the receiver listens for their reflection from a target in its path. The distance (d) of the target is measured based on the time delay (t) for the reception of the transmitted sound pulse with speed (s) according to Eq. (5.1). It is a four pin sensor that has an easy Micro Controller Unit (MCU) interface. It is powered using a regulated 5v supply through the Power (Vcc) and Ground (GND) pins of the sensor. The trigger and the echo pins are connected to the GPIO pins of the Raspberry pi and used to control the sensor. A high signal at the trigger pin for a minimum duration of $10\mu s$ initiates the sensor to transmit eight ultrasonic pulses and a high signal is generated at the echo pin, when a reflection is received. The time difference between high signal generated at the trigger pin and the time at which a high signal was received at the echo pin is used to calculated the distance of the target. The distance is calculated based on Eq. (5.1) but the result is divided by two in-order to obtain the correct distance of the target. This is because the time delay calculated is for the signal to travel back and forth. The sensor has a resolution of about 0.3cm.

$$d = s * t \tag{5.1}$$

IWR1642 Configuration and Processing

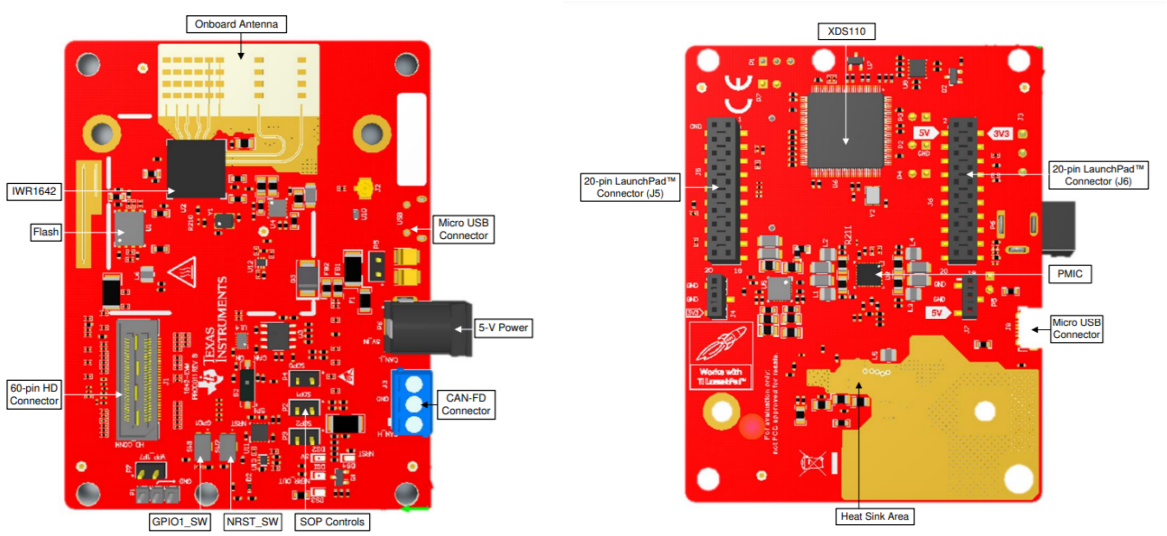

(a) Front-View (b) Rear-View

Figure 5.7: IWR1642 BOOST EVM [62]

The IWR1642 is a single chip mmWave sensor based on FMCW radar technology that can operate in the 76 to 81GHz band to determine the range, velocity, and angle of targets within its FoV. The sensor simplifies the implementation of a mmWave radar system by integrating Radio Frequency (RF) radios, clocking, Analog-to-Digital Converter (ADC), ARM R4F-based MCU and C674x Digital Signal Processor (DSP) and solves the challenge of discretely implementing the required components of radar system. This results in reduced power consumption and cost. The MCU and the DSP with integrated peripherals such as UART, and Controller Area Network (CAN), enable flexibility of the sensor to be tailored for real-time applications. The sensor belongs to the industrial range and it is used over the automotive range as it is cheaper. They are similar in hardware specifications apart from the lack of additional qualifications, for use in commercial automobile and additional fast CAN interfaces that are not required in bicycles. The IWR1642 boost module is used in this project and is shown in Fig. 5.7. It is an IWR1642 sensor evaluation board with a small form factor, that contains everything required to start developing applications along with a Software Development Kit (SDK) that enables faster and easier prototyping.

The configuration and setup of the radar according to the project requirements using the SDK involves two main tasks namely front-end radio configuration and back-end signal processing responsible for the radar functioning. The front-end configuration involves the tuning of the RF radio and the analog sub-system for the transmission and the reception of the radar frames. The back-end processing encapsulates all the data processing of the RX signal to extract useful information of the reflected targets. It consists of taking ADC samples post analog filtering from the radar front-end as

input and producing the necessary information of interested targets to reduce redundant computation and data transfer to the threat assessment block implemented in the Raspberry pi controller. The RF front-end configuration and the data transfer to the Raspberry pi controller for threat assessment is implemented in the ARM R4F MCU integrated in the sensor. The back-end processing of the raw RX signals is implemented in the integrated C674x DSP. The construction of the TX frames using FMCW chirps and tuning of the analog RX signal processing chain, define the detection capability of the radar.

Front-end Configuration: The front-end block is shown in Fig. 5.8. The configuration of the TX signal can be categorised into three steps namely profile, chirp, and frame. The profile is a template for a chirp and consists of various parameters that are associated with the transmission and reception of the chirp. A chirp type is associated with a profile and inherits all the properties of the profile and additionally includes information on the TX antennas on which it should be transmitted. The Frame is constructed by defining a sequence of chirps using the previously defined chirp types. The TX frame for the project, is configured to achieve maximum detection range and velocity with minimal power and computational complexity. This was considered according to the system requirements mentioned in Section 2.1. The higher detection range of faster vehicles enables the system to generate on-time warnings on a wider range of scenarios.

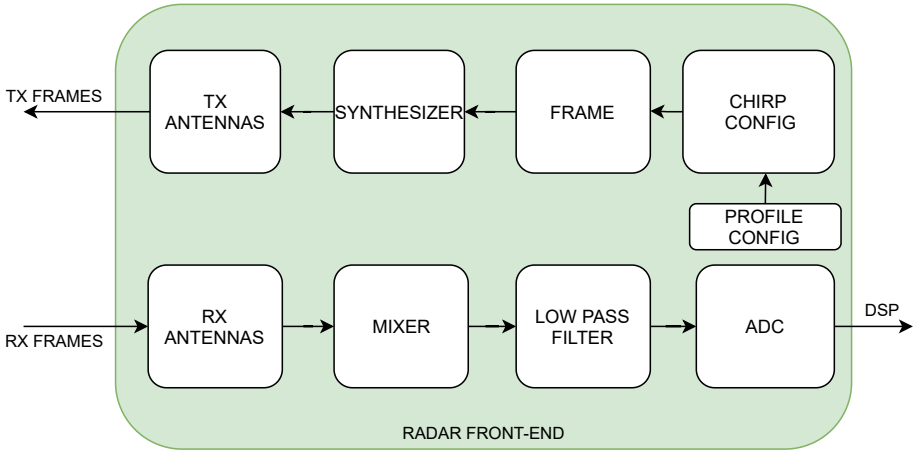

Figure 5.8: Radar Front-end

1. **Maximum Range:** The maximum range of detection depends on the Signal to Noise Ratio (SNR) of the reflected signals from targets and the maximum IF Bandwidth IF_{BW} supported by the radar. The relation of maximum range (R) with the IF_{BW} is considered for configuring the parameters of the FMCW chirps used in the construction of the TX frames according to Eq. (5.2), where S is the slope of chirp and c is the speed of light.

$$R_{max} = \frac{IF_{max} * c}{2 * S} \tag{5.2}$$

$$IF_{BW} = 0.9 * ADC_{Sampling} \tag{5.3}$$

The configuration used in the project theoretically enables a maximum range of 120m in complex 1x operation mode and is shown in Table 5.1. The imaginary part of the RX signals that contains the interference information are filtered using the front-end filters in complex 1x operation mode. This results in twice the useful IF frequency and maximum range as only the real IF spectrum is sent to the ADC. The IF_{max} is fixed to 4.5 MHz, slight under the maximum available bandwidth of the sensor used, which is 5MHz due to the limited on-chip memory of 1.5MB. This fixing of the IF_{max} results in an ADC sampling rate of 5000ksps according to Eq. (5.3). Which in turn results in the chirp frequency slope of 5.6MHz/μs to achieve a theoretical range of 120m according to Eq. (5.2). This slope reduces the chirp bandwidth (B) and enables a reduced range resolution of 36cm according to Eq. (4.4). This range resolution is inferred to be more than enough for the project, as the targets of interest are mainly vehicles like cars and bicycles that are practically not expected to be more closer to each other due to their size. Even if they are in some rare scenarios, they are expected to be resolved in the velocity direction due to their difference in speed. Furthermore, the disability to resolve them as separate targets is also inferred not to affect the performance of the warning system, and the longer detection ability is considered more important to generate early warnings. The one shortcoming of the reduced resolution is the disability to provide rich point cloud of objects in closer range, as it is also important for the warning system to be aware of objects that are present below the MSD. It is possible to work around this trade-off by having another configuration tailored for high resolution targeting a shorter distance and including it in the TX frame. This will enable multi-mode capability and improve the detection performance, but will also result in increased number of chirps, increased power, and increased back-end processing as separate processing paths must be defined for each configuration. Thus, it is inferred not to be suitable for the current project. The effect of this shortcoming on the system performance is not expected to be significant and is addressed in Section 6.3.2. The frames are also configured to transmit on both the TX antennas available in the sensor simultaneously to achieve an improved SNR of target reflections within 120m in the main focused FoV of the radar. This is inferred to enable easier removal of noise and better detection of desired targets in the back-end processing.

Parameter	Value
Start Frequency (GHz)	76.01
ADC start time (μs)	4.8
Ramp end time (μs)	56
Number of ADC samples	256
Frequency slope (MHz/μs)	5.6
ADC sampling frequency (MHz)	5
Bandwidth (MHz)	409

Table 5.1: Radar front-end configuration

2. **Maximum Velocity:** The maximum detectable velocity of targets depends on the time between the start of two consecutive chirps in the TX frame, which includes the chirp time and the idle time. The idle time is the time between the end of a chirp and the beginning of the next chirp, this constitutes the time for the synthesizer to ramp down. The chirp parameters configured to achieve a long detection range of 120m limits the maximum detectable target velocity to approximately 14m/s for 128 chirps, according to Eq. (5.4), where T_c is the total chirp time and λ is the wavelength of the chirp. This is because the velocity estimation is dependent on the phase difference as described in Section 4.3 and is unambiguous only if the difference is within $\pm 180°$. The maximum detectable velocity extension enabled configuration is used for the project. This extension results in the construction of the TX frame with two different idle times $3\mu s$ and $14\mu s$ respectively as in Fig. 5.9 for 128 chirps. The chirps with the lower idle time will have lower chirp repeat periodicity which results in higher maximum unambiguous velocity as compared to the slow chirps according to Eq. (5.4). The target velocity is estimated from both the chirps along with the Chinese remainder theorem in the back-end processing and enables upto 3 times higher maximum velocity than the native maximum velocity [63]. This is done to improve the capability of the warning system to also perform well and provide on-time warnings in highway traffic scenarios, where the velocity of target vehicles are high. It is considered to be important for the system due to the reduced speed of bicycles with respect to the speed of interested targets such as cars.

$$V_{max} = \frac{\lambda}{4T_c} \tag{5.4}$$

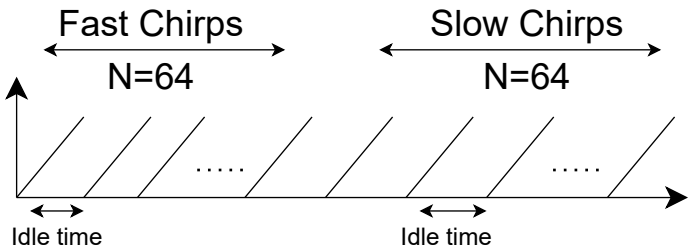

Figure 5.9: Radar Tx Frame

Back-end Processing: The block diagram of the back-end radar processing chain used in the project is shown in Fig. 5.10. The input from the front-end channels are obtained in the DSP and range FFT followed by Doppler FFT is performed on the RX chirps corresponding to the chirping pattern on the TX antenna, to obtain the range and velocity estimates as mentioned in Section 4.2 and Section 4.3. This results in discrete reflection points that are separated in range and velocity. These points are then pruned by CFAR detection and peak grouping for the range and velocity estimates. The CFAR is an adaptive detection algorithm used to remove interference, ground clutter and redundant reflections from actual target reflections, and minimise further computation [64]. The configurations used for CFAR detection are shown in Table 5.2.

A detected reflection has to have a power more than the threshold computed by the CFAR algorithm, in both the range and velocity direction, in order to become a

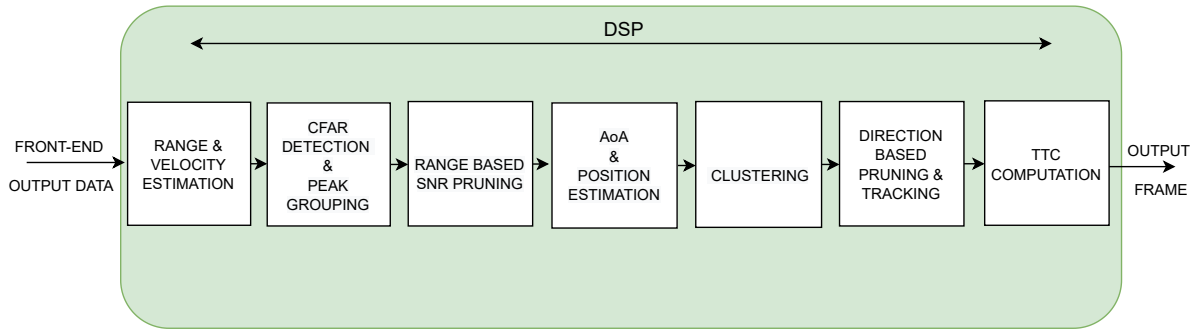

Figure 5.10: Radar Back-end Processing Chain

Parameter	Range	Doppler
Average Mode	CASO - CFAR	CA - CFAR
Window Length	8	8
Guard Length	4	4
Threshold Scale	12 dB	12 dB

Table 5.2: CFAR - Configuration

valid detection point for further processing. The Cell Averaging Smallest Of (CASO)-CFAR uses the smallest noise-floor of the bins higher and lower than the bin under test for computing the power threshold and is used in the range direction. This is done to minimise the over-filtration of reflections from desired targets, as it is the initial stage of filtration, which may result in reduced detectability of the radar. This is followed by Cell Averaging (CA)- CFAR in the velocity direction. It uses the average noise-floor of the bins higher and lower to the bin under test to compute the power threshold. The determined noise power is multiplied by a threshold scaling factor for determining the detection threshold. The threshold scaling factor is one the key parameter that affects the detectabilty of desired targets from background clutter and needs to be carefully assigned for the CFAR algorithms in both the range and velocity directions. This factor is set by taking the RCS of the desired targets and the operating environments of the warning system into account, using the SNR based radar range equation given in Eq. (5.5). The RCS is the measure of the ability of a target to reflect radar signals in the direction of the radar receiver and depends on various factors such as physical dimensions of the target, electrical properties of the target surface, and the frequency of the radar transmitter. The computational determination of the RCS is possible only for simple targets. The other parameters of the radar taken for the calculation based on the configuration used are given in Table 5.3.

$$R_{max,SNR} = \sqrt[4]{\frac{P_{tx} G_{tx} G_{rx} (\lambda)^2 \sigma T_c N_c N_{txrx}}{(4\pi)^3 K T_e \eta L \; SNR}} \tag{5.5}$$

Parameter	Value	Parameter	Value
Tx Power p_{tx}	-12.5 dBm	Ambient Temperature T_e	290 K
Tx Antenna Gain G_{tx}	44 dB	Chirp Time T_c	75.89μs
Rx Antenna Gain G_{rx}	44 dB	Bandwidth B_r	4.5 MHz
Total Antennas $N_{tx}N_{rx}$	4 dB	Number of Chirps N_c	128
Wavelength λ	0.0038961 m	Noise Figure η	15dB
Boltzmann's Constant k	1.38 * 10^{-23}	System Loss L	12dB

Table 5.3: Maximum Range Parameters

The variation of the minimum SNR of the reflected chirps with respect to range for different RCS values corresponding to the desired targets such as pedestrians, bicycles, cars, and trucks in an environment with minimal loss is shown in Fig. 5.11. Cars and trucks have a relatively higher RCS for the mmWave radar, which is approximately standardised to be 5 sq.m and 100 sq.m respectively. Where as, the approximation of the RCS value of bicycles has not been standardised with on-going research [65]. Thus, the RCS of bicycles was assumed to be in the range of 1.5 sq.m, based on the inference that it is not as high as cars but higher than human adults which is 1 sq.m due to the presence of the cyclist while riding. Bicycles have the least RCS among the desired targets that have a relatively higher maximum speed and require a longer detection range for on-time warnings. It can seen that they theoretically have a SNR of 12 dB at 70m beyond which it detiorates further. This detection range of bicycles was considered more than enough for the warning system to provide on-time warnings, even if there is a decrease in actual road environments, where the loss is higher. This inference was based on considering the maximum relative speed of bicycles. Thus, the threshold value of 12dB is concluded to be ideal to minimise the low confident false detections and provide maximum detection range.

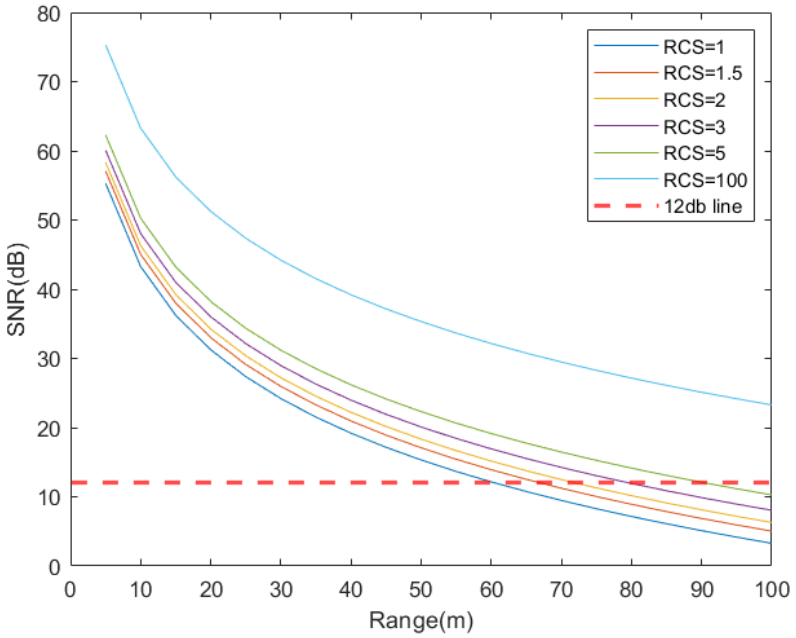

Figure 5.11: Range Vs SNR

The peaks in range and Doppler direction are grouped together and represented by the highest one, after the CFAR- detection to reduce the number of points from a single target. This reduces the computation per frame and enables processing of points only with strong unambiguous peaks that have the higher signal strength. The detected peaks are further pruned based on their range and SNR to eliminate nearby clutter that may have resulted due to the lower CFAR threshold for distant detection of bicycle targets. The SNR thresholds are set for three range groups with higher requirement for close by detections as shown in Table 5.4. The thresholds were determined based on the inference from Fig. 5.11 and a few field trials. The minimum range group was set only from 0.4m, due to the range resolution of the front-end configuration used. The angle of the pruned points are then estimated as described in Section 4.4 and the position of each points are mapped as X and Y locations in metres with the radar position as the origin, based on their range and angle information. This mapping makes further processing and interpretation of the radar output data frames simpler.

Range groups	SNR threshold
0.4 to 10 m	16 dB
10 to 30 m	15 dB
Above 30 m	12 dB

Table 5.4: Range Based Pruning

Clustering is performed on the positioned point data using the Density Based Spatial Clustering of Applications with Noise (DBSCAN) algorithm [66] to essentially reduce the number of points provided to the tracking algorithm and introduce hysteresis, so that only track one point from a target is tracked, and does not switch between adjacent targets. The algorithm groups together a minimal number of points separated by a minimum distance and speed. It was considered critical for the project, as the desired targets such as cars have a relatively high RCS, which increases the probability of multiple strong points reflected from the same target. The tracking of each point will result in redundant computation and reduced tracker performance. The output of the clustering algorithm is a mean location of the clustered points and its margin locations assuming the shape to be a rectangle. The used configuration of the algorithm is shown in Table 5.5. The key parameters in the configuration are the maximum distance between the points epsilon and the minimum number of points in a cluster. Epsilon is fixed at 2.5m considering the dimension and size of cars, as they are assumed to be the most common desired targets. A higher value considering the properties of trucks will result the majority of objects to be grouped in the same cluster when they are located close to each other. The minimum number of points is fixed at 1 and the maximum points in a cluster is set to 4. This was done to enable the detection of the weaker targets such as bicycles at higher ranges, as their detection points may reduce with increase in their distance from the radar. This is due to the reduced range resolution of the chirp configuration and peak grouping. The strongest point in the cluster is provided as the representative point to the tracking algorithm.

Parameter	Value
Epsilon	2.5 m
vFactor	3 m/s
MinimumPointsInCluster	1
Neighbours Limit	4
Maximum Clusters	32

Table 5.5: DBSCAN - Configuration

The tracking algorithm is a standard Extended Kalman Filter with four states X-position, Y-position, relative velocity along X direction, and relative velocity along Y-direction. It was used to improve the stability of the target detection at longer distances, which translates to a improved performance of the warning system. It enables to eradicate false detections caused by other targets that are out of interest and noise present on real road scenarios. These signals will cause the warning system to misinterpret them as interested targets and result in higher false warnings. In addition to this, further pruning is done by only tracking targets that are within the longitudinal range of 2m or is moving towards the host bicycle in the longitudinal direction. This was done as only these targets contribute to the rear-warning detection of the radar. The objects that are moving away from the bicycle or travelling with the same relative velocity are eliminated as they will have a very high TTC value and detecting them introduces redundancy. The movement of the target towards the bicycle is detected by the negative sign of the target velocity, which resulted due to the anti-clockwise movement of the IF signal phasor for positive target velocity relative to the bicycle. This pruning enables to reduce the false detections of the radar due to external noises significantly and provides a stable detection of targets with reduced redundant computational load. The TTC of the tracked objects is calculated using their longitudinal range and the relative velocity. The properties such as position in lateral and longitudinal direction with reference to the radar, along with its TTC is populated on the output frame that is shipped to the external Raspberry pi controller of the warning system. The format of the output frame of the radar is shown in Fig. 5.12 and its size depends on the number of useful targets detected to enable fast and reliable communication to the external Raspberry pi controller through the UART peripheral. The amount of time needed by radar chain to process input point cloud and deliver target information is a function of number of targets currently tracked, and number of radar front-end measurements received. Since the number of targets tracked are pruned significantly, the controller was able to process and deliver information faster across a wide range of noisy road scenarios.

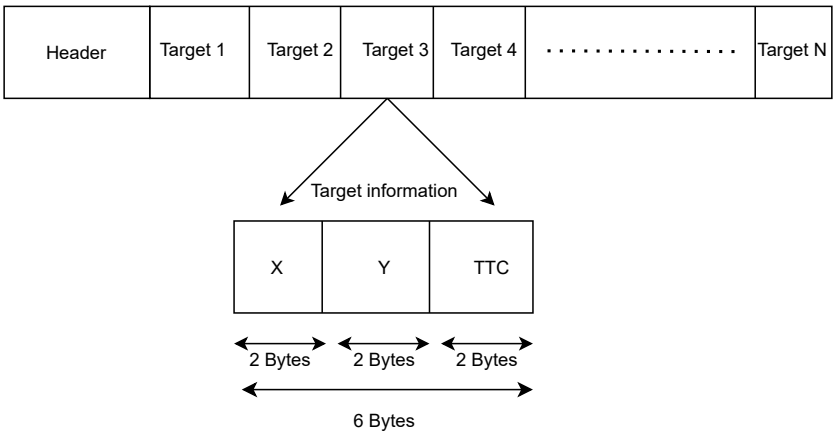

Figure 5.12: Radar Output Frame

5.2.2 Threat Assessment

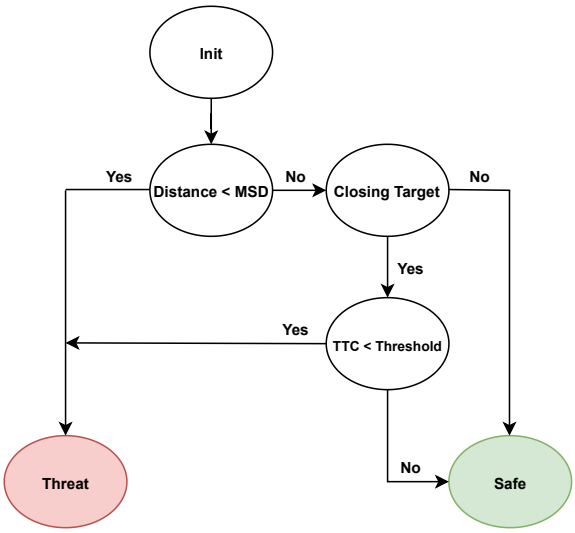

Figure 5.13: Threat Assessment Method

The designed algorithm is a deterministic based approach utilising two metrics, namely TTC and MSD for threat assessment. TTC is used as the metric to estimate the hazard of distant closing targets that are approaching from behind and the MSD is used to evaluate the hazard of targets present in close proximity on the rear and the side surroundings of the host bicycle. This enables to utilise the high correlation of TTC metric to the human-decision of performing the lateral maneuver and also compensate its shortcoming mentioned in Section 3.2.3, for the assessment of closing targets from behind. This is inferred to enable an accurate and acceptable threat estimation. The TTC metric enables to evaluate a threat based on the the reaction time that the vehicle in target side has to avoid collision, if it travels in the same path and the host bicycle interfered in it as a result of the lateral maneuver. The MSD metric enables to evaluate a threat based on the minimum longitudinal distance to be maintained to provide minimal reaction time for the vehicle in target side has to avoid collision and to detect targets that restrict the lateral displacement of the maneuver on the sides. The mathematical representation of

these metrics are shown in Eq. (5.6) and Eq. (5.7), where (D) is the minimum spatial distance, Δx is the spatial distance between the bicycle and the target, and Δv is the relative speed of target with respect to the host bicycle.

$$TTC = \frac{\Delta x}{-\Delta v} = \frac{x_l - x_f}{v_f - v_l} < TTC_{threshold} \tag{5.6}$$

$$D < MSD \tag{5.7}$$

The threat assessment is carried out in one fold for the targets in the rear-side blind-spots and in two fold for the closing targets from behind as shown in Fig. 5.13. A detected target on the rear-side blind-spots is only checked for its presence within the characterized MSD and is assessed as a threat if it is, else it is assessed to be safe. This is not the case for a closing target from behind. A target from behind is initially checked for its presence within the characterized MSD, it is directly assessed as a threat if it is, else its TTC is also compared to the $TTC_{\text{Threshold}}$ before assessing it to be safe. The $TTC_{\text{Threshold}}$ of 6sec was set based on the experimental results obtained for a LCDAS in cars [59] and the MSD was set to 2m in the rear based on the inference from few related literature. The lateral distance of 3m on either sides was considered as the region of interest and only targets violating the characterised MSD and $TTC_{\text{Threshold}}$ within this region are evaluated as threats in the rear. This region is specified considering the average lateral displacement possible during lateral maneuvers across different road-scenarios. The specification of this region of interest is done to minimize the false positives generated from targets that are not considered to affect the lateral maneuver. The MSD for the rear-side blind-spot sides also need to be set to 3m according to the specified region of interest in the rear. But this increased distance resulted in increased false warnings in some road scenarios and was deemed not to be ideal. This inference was obtained by mounting the setup on the bicycle and testing it on real road scenarios as shown in Fig. 6.2. From the test results, it was inferred that the value of the MSD for the sides, needs to varied for different road scenarios. For example, in a road with small bicycle lane that has cars parked throughout the sides, the value of MSD must be low to prevent unnecessary warnings resulting due to the cars parked in the sides. Similarly in a wide bicycle lane scenario, a higher MSD is needed, as higher lateral displacement is possible during the maneuver. To address this trade-off the MSD was set according to the scenarios with minimal lateral displacement possibility to keep the false warnings minimal across all road scenarios. The effect of this trade-off on the system performance is described in Section 6.4. These configured values for the threat assessment provide acceptable performance with some limitations and can be tuned based on further investigation if necessary.

5.2.3 Warning Algorithm

The warning algorithm defines how and when warnings are generated by the system based on the threats assessed in the surrounding environment as shown in Fig. 5.14. The warnings generated by the system is a tuple containing two information. The first information denotes the direction of a potentially dangerous maneuver that must be indicated to the host cyclist, based on which the cyclist can avoid the maneuver. The direction of the warnings are determined by the ultrasonic sensor direction and the lateral position information of targets obtained from the mmWave radar. The Fig. 5.15 shows how the warning direction is determined based on the position of the closing target from

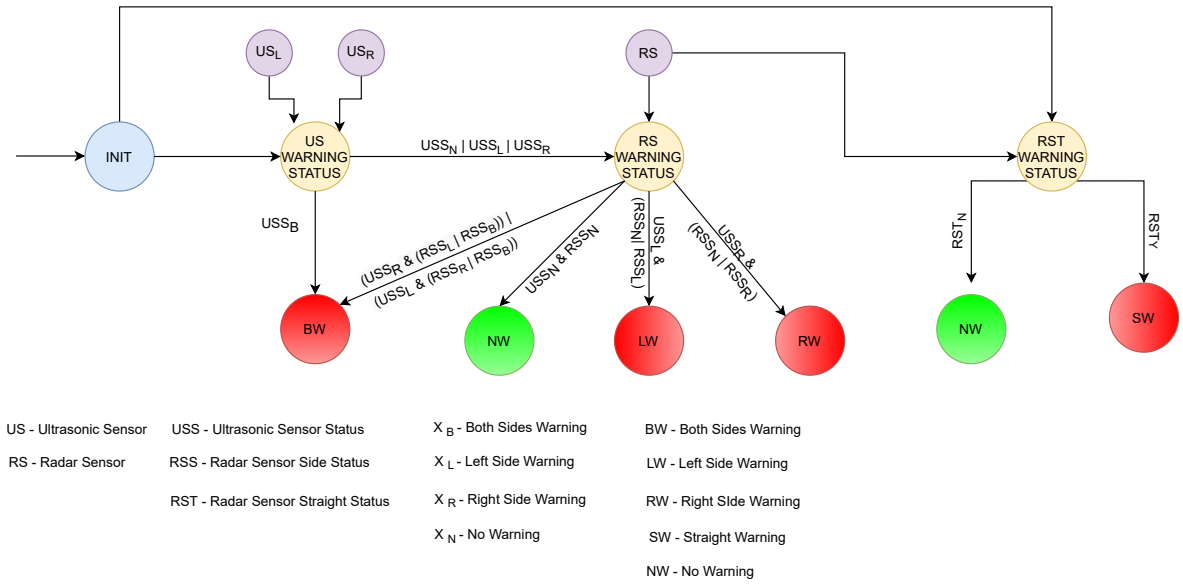

Figure 5.14: Warning Algorithm

behind. As mentioned in Section 5.2.2, the region of interest for closing targets is specified to be a lateral distance of 3m on either sides. This region of interest is classified into three direction as shown in Fig. 5.15, based sub-regions based on the lateral distance from the bicycle, which constitute the virtual adjacent lanes. The second information denotes that a hazardous vehicle is approaching right behind the bicycle and can be used to alert the driver of the approaching vehicle to be aware of the host bicycle to avoid collision. This may conveyed through the means of a light signal present in the rear of the bicycle. This additional information is expected to enable improved cycling safety by preventing possible rear collisions even in an environment, where not all vehicles are equipped with the same type of assistance systems.

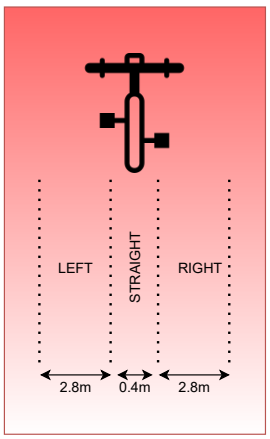

Figure 5.15: Closing Target Virtual Direction Separation

Chapter 6

Testing and Results

The testing procedures that were carried out along with their results are mentioned in this section. The mounting of the system along with the sensors on the bicycle is shown in Fig. 6.1. The radar module is mounted firmly on the rear carrier of the bicycle using nylon cable ties, the Raspberry pi is stuck to carrier using a double side tape, and the ultrasonic sensors are also stuck to sides using the double side tape. The ultrasonic sensors are mounted at a height from the ground, to minimise ground reflections. Their performance of detection is inferred not to be affected by this as the targets of interest are taller than this height.

(a) Rear view (b) Side view

Figure 6.1: System Mounting on Bicycle

6.1 Ultrasonic Sensor Performance

The ultrasonic sensors were installed on both the sides of the bicycle rear wheel as shown in Fig. 6.2b with an arduino MCU, and a LCD display in the front handlebar as shown in Fig. 6.2a to view the measured distance on both the sides in real-time. The bicycle with this setup was ridden around in different road scenarios and measured distances on

the sides in different scenarios was analysed to decide on the suitable MSD as mentioned in Section 5.2.2.

(a) LCD Display Mounting (b) Ultrasonic Sensor Mounting

Figure 6.2: Ultrasonic Sensor Field Trial Setup

Their accuracy and capability of detection was also analysed. They were observed to detect with a good accuracy and stability at different distances. A variety of tests were conducted in indoor and outdoor conditions. It was inferred that they have a good sensing capability but are highly restricted to their line of sight, which is not seen to affect the warning system performance. Tests were also conducted by placing a target at different known distance from the sensor, ranging from 0.05m to 1m and its estimation was observed over time. This resulted in highly stable performance with minimal deviation as shown in Fig. 6.3.

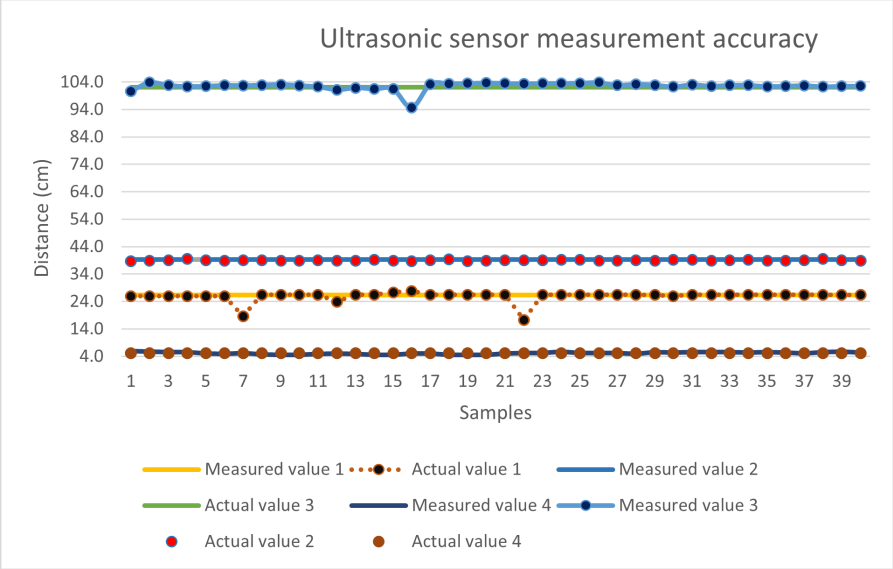

Figure 6.3: Ultrasonic Sensor Measurement Analysis

6.2 mmWave Radar Performance

The performance of the mmWave radar was evaluated with respect to maximum range of detection, and accuracy of detection in different real road scenarios and lighting conditions. The tests were carried out by mounting the radar sensor in the rear of the bicycle and connecting it to a laptop using USB-UART interface, which stored the received radar frames and also plotted the values in real-time using a matlab Graphical User Interface (GUI). The GUI was provided by Texas Instruments, and was modified to receive and plot frames according to the project configuration. The laptop screen was mirrored to a mobile phone mounted on the handle bar of the bicycle using team-viewer remote connection application which enabled to evaluate the detection capability of the radar sensor to an extent in real-time. The screen seen in the mobile phone is shown in Fig. 6.4. In addition to this, another mobile camera was mounted on the rear to record the rear-environment to be aware of the ground truth.

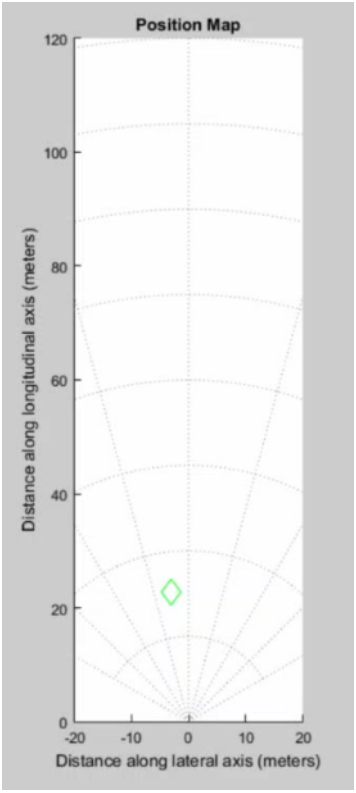

Figure 6.4: mmWave Radar Visualization Screen

6.2.1 Detection Range in Different Road Scenarios:

The range of detecting the targets of interest such as bicycles, cars, and scooters is an important parameter that influences the performance the warning system. Thus it is important to evaluate this parameter in different real-road scenarios. The detection capability of the radar sensor was evaluated in three common road scenarios including dedicated bicycle lane, shared road with bicycle lane marking, and shared road without lane marking.

(a) Shared Road Without Lane Marking

(b) Dedicated Bicycle Lane

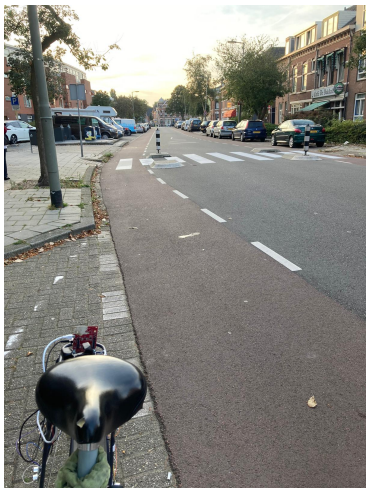

(c) Shared Road With Bicycle Lane Marking

Figure 6.5: Road Scenarios

1. **Shared Road Without Lane Marking Scenario:** This scenario is referred to scenarios, where there is no dedicated bicycle lane and all road users share the same space. These scenarios are commonly found in interior streets. The test was conducted in such scenarios with multiple non-interested targets present as shown in Fig. 6.5a. This was done as this scenario is inferred to have the most possibilities of highly noisy environments. The Fig. 6.6a shows the range in which 15 bicycles were detected in this road scenario. The average range of detection is around 36.3 m. Most of the bicycles were detected around 37 - 40 m with three exemption. Two of which were detected at a maximum distance of 43 m and one with the minimum distance of 21 m. These results are seen to be encouraging for the warning system as the detection ranges are quite high under noisy scenarios and would be more than sufficient for the warning system to detect threats under 6 sec as the speed of the targets are not expected to be very high in these scenarios. Cars were not considered in this scenario as only a few of them were present during testing and further they are inferred to have much higher ranges due to their higher RCS properties.

2. **Dedicated Bicycle Lane Scenario:** This scenario is referred to scenarios, where there is a dedicated bicycle lane which is physically separated from the road infrastructure of other users such as cars and trucks. These scenarios are commonly found in highways and in some main roads. The test was conducted in one such scenarios as shown in Fig. 6.5b. The Fig. 6.6b shows the range in which 10 bicycles were detected in this scenario. The average range of detection is around 42.6m. Most of the bicycles were detected around 40 and 45m with three exemptions. Two of which were detected at a maximum distance of 54m and 50m and one with the minimum distance of 28m. These results are seen to be encouraging for the warning system and have a relatively higher detection range as the number of non-interested targets are minimal which reduces the noise in the environment.

3. **Shared Road With Bicycle Lane Marking Scenario:** This scenario is referred to scenarios, where there is a bicycle lane separated with lane markings and not physically separated from the road infrastructure of other users such as cars and

trucks. These scenarios are commonly found in cities. The test was conducted in one such scenarios as shown in Fig. 6.5c. The Fig. 6.6c shows the range in which 15 bicycles and cars were detected in this scenario. The average range of detection is around 27 m for bicycles and 60 m for cars. Most of the bicycles were detected around 28 and 33 m with five exemptions that were detected at a minimum distance of 21 and 22m. The majority of the cars were detected around 60 to 70m with few exemptions around 40 to 55m with 40m being the minimum distance. These results are seen to be relatively lower than the other scenarios as the test position was on a slightly curved path as seen in Fig. 6.5c. In-spite of this restriction of the TX frames to travel longer as they travel in a straight line, the results still show a good range for cars but a reduced range for bicycles. The only drawback of this reduction is the restriction to only provide timely warnings for bicycles with a maximum relative speed of 6.5 m/s, which is very high and not inferred to occur commonly.

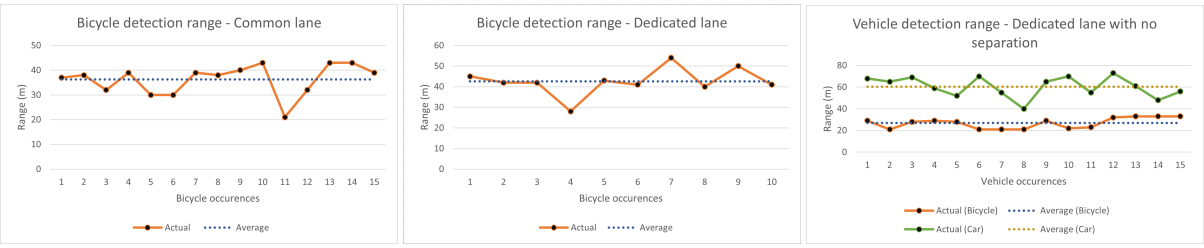

(a) Shared Road Without Lane Marking

(b) Dedicated Bicycle Lane

(c) Shared Road With Bicycle Lane Marking

Figure 6.6: Detection Range Plot

6.2.2 Accuracy of the mmWave Radar:

The accuracy of the range and velocity estimated by the radar was verified using the Matlab GUI, a mobile phone with apple measure application [67], and Walfort wireless bicycle computer [68]. The range was initially measured using the mobile application and the radar was used later to estimate the range of a bicycle target placed at the same point. The radar estimate and the measured range were compared and verified to be almost similar as in Fig. 6.7a. Similarly, a target bicycle was installed with mobile computer and was ridden towards the stationary radar at different velocities and their corresponding radar estimates were compared. The radar estimate and the velocities measured by the bicycle computer are comparable as the radar is stationary and the relative velocity estimated is equal to the target velocity. The estimates and the measured values were verified to be almost similar as shown in Fig. 6.7b.

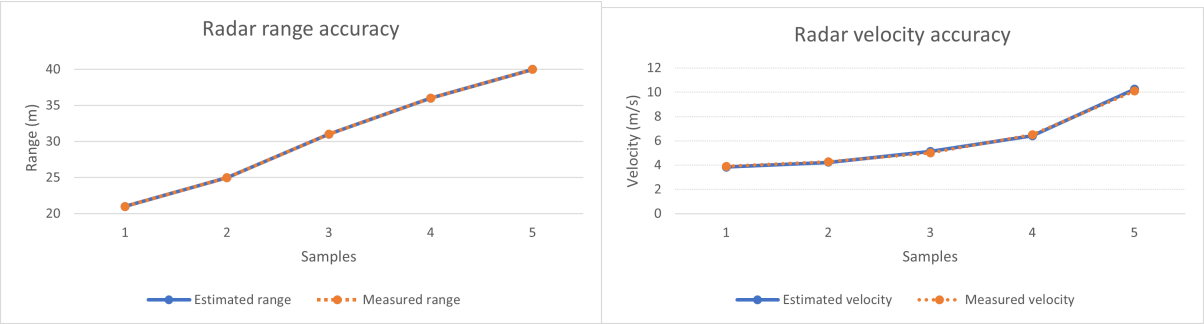

(a) Range (b) Velocity

Figure 6.7: Radar Accuracy

6.3 Lateral Maneuver Warning System

The evaluation of the overall warning system was carried out in two fold. It was initially tested by adapting procedures followed in the ISO 17387 standard for LCDAS in cars [9]. This is done as the system functionalities are quite similar with change in the targets and operating environment. The system was later installed on a bicycle along with a mobile camera to record the video of the environment and ridden around in different road scenarios. The status of the warning system was continuously displayed on a mobile phone remotely connected with the Raspberry pi and also logged and stored in a csv file with timestamp. The stored file was later used to compare with the frames captured by the camera to cross check the ground truth.

6.3.1 ISO 17387 Testing Procedure:

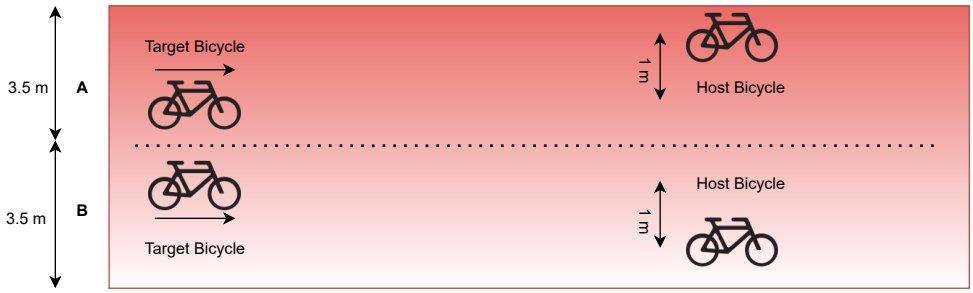

Figure 6.8: Test Scenarios

The purpose of this test is to check whether the system works according to its design. The testing procedure includes a scenario in which a target bicycle approaches the host bicycle with the warning system at different speeds. The procedure was carried out in a separated bicycle lane and tested on either sides as shown in Fig. 6.8. The test was repeated for 3 times in each direction and the system was able to generate warnings accordingly in all cases. The distance at which the system generated the warning for each speed of the target bicycle is shown in Table 6.1. The false warning test was also conducted and verified that the system did not generate warnings for vehicles present beyond the configured lateral distance of 3 m on either sides.

Target Velocity (m/s)	Warning Distance (m)	Warning Timing (s)
4.5	24.5	5.4
5.5	24.6	4.5
9.7	43.8	4.5

(a) Left side

Target Velocity (m/s)	Warning Distance (m)	Warning Timing (s)
4.0	22.2	5.5
5.5	25.1	4.5
9.0	39.2	4.4

(b) Right side

Table 6.1: ISO 17387 Testing results

6.3.2 Real-time Scenario Testing:

The purpose of this test was to evaluate the performance of the warning system in different road scenarios. The bicycle was ridden across all the 3 different road scenarios mentioned above for a total duration of around 32 minutes of which around 15 minutes was in shared road with and without lane marking and the remaining duration was in dedicated bicycle lane scenario. The warnings generated by the warning system stored in the csv file were later compared to camera frames obtained and verified. Then a confusion matrix was used to describe the performance of the warning system using the metrics given in Table 6.2.

The basic terms used for the construction of the confusion matrix are defined as follow:

- True Positive (TP): The cases in which the system generated a warning in a particular direction and a possible obstacle was found in same direction on the camera frame at the same point in time.
- True Negative (TN): The cases in which the system generated no warnings and no possible obstacle was found on the camera frame at the same point in time.
- False Positive (FP): The cases in which the system generated a warning but no possible obstacle was found on the camera frame at the same point in time.
- False Negative (FN): The cases in which the system did not generate a warning but possible obstacles were found on the camera frames at the same point in time.

Performance Metric	Definition	Formula
Accuracy	It denotes the overall correctness of the warning system.	$\frac{TP+TN}{total}$
Misclasification Rate	It denotes the overall incorrectness of the warning system.	$\frac{FP+FN}{total}$
Sensitivity	It denotes the proportion of cases in which the warning system generated a warning correctly.	$\frac{TP}{Actual\ "YES"}$
FP Rate	It denotes the proportion of the cases in which the warning system generated a warning incorrectly.	$\frac{FP}{Actual\ "NO"}$
Specificity	It denotes the proportion of the cases in which the warning system did not generate a warning correctly.	$\frac{TP}{Actual\ "YES"}$
Precision	It denotes the success probability of the warning system in making a correct warning decision	$\frac{TP}{Predicted\ "YES"}$

Table 6.2: Performance Evaluation Metrics

Individual Scenario Performance: The performance of the system is evaluated by grouping together the shared road with and without lane markings scenarios, where the number of road users are high and separately for the dedicated bicycle lane scenario with a relatively lower number of road users. This is done to give a comparison of the system performance in a noisy environment and an environment with relatively lower noise. The confusion matrix for both the cases is given in Table 6.3 and Table 6.4.

The performance of the system in both the cases is shown in the Table 6.5. In both cases, it is obvious that the system has a high level of accuracy (above 90%). However, the most noticeable difference is the sensitivity, which is an essential statistic that indicates the true effectiveness of the warning system by indicating its capacity to identify threats. It is considerably good under dedicated bicycle lane scenario, but falls short to an extent in shared road scenarios. This degradation is inferred to be mainly due to the high sampling rate of the warning system, the radar configuration and the threat assessment

		Prediction outcome		
		p	**n**	**total**
actual value	**p′**	203 TP	98 FN	301
	n′	11 FP	1123 TN	1134
	total	214	1221	

Table 6.3: Confusion Matrix - Noisy Road Scenarios

		Prediction outcome		
		p	**n**	**total**
actual value	**p′**	142 TP	25 FN	167
	n′	27 FP	1718 TN	1745
	total	169	1743	

Table 6.4: Confusion Matrix - Dedicated Bicycle Lane Scenario

thresholds. The configuration of the radar to enable long range detection restricts it to detect objects that are very close to the bicycle in the rear and leads to a very small region out of coverage of the system between the radar and the ultrasonic sensors. Thus, warnings for an approaching vehicle are stopped a little earlier when the vehicle is in the out of coverage region itself before coming under the threshold coverage of the ultrasonic sensor or passing the host bicycle. This out of coverage region is very small and its effect is not as significant in the dedicated bicycle lane scenario as the duration of the presence of target vehicles in the out of coverage region was very minimal due to the higher relative speed of vehicles. Whereas, the effect is significant due to the reduced speed of vehicles in shared road scenarios. This effect can be improved with a slight increase in the sampling time of the warning system but it may result delayed warnings is some cases. Thus, an ideal solution would be to only clear the warning status of the system when no warnings are generated for 2 or 3 consecutive samples. This is inferred to improve the sensitivity of the system significantly but with an slight increase in the FP rate. The characteristics of the mode of the communication used to intimate the rider along with this trade-off needs to be considering when improving further.

Performance Metric	Shared Road Scenario	Dedicated Bicycle Lane Scenario
Accuracy	92.4 %	97.3 %
Misclasification Rate	7.6 %	2.7%
Sensitivity	67.5 %	84.4 %
FP Rate	1 %	1.5 %
Specificity	99 %	98.4 %
Precision	94.9 %	84 %

Table 6.5: Performance Metrics - Individual Scenario

Overall performance: The overall performance of the system across all the different road scenarios is evaluated in this section. This is done to give a description of the system performance along with the time in advance it was able to generate warnings for approaching vehicles. The confusion matrix for the evaluation is given in Table 6.6.

		Prediction outcome		
		p	**n**	**total**
actual value	**p′**	345 TP	123 FN	468
	n′	38 FP	2841 TN	2879
	total	383	2964	

Table 6.6: Confusion Matrix - Overall Performance

Performance Metric	Overall
Accuracy	95.2 %
Misclasification Rate	4.8 %
Sensitivity	73.7 %
FP Rate	1.3 %
Specificity	98.6 %
Precision	89.6 %

Table 6.7: Performance Metrics - Overall System

The overall performance of the system is shown in the Table 6.7. It can be inferred from the results that the warning system performs well across different road-scenario with

a good accuracy and an acceptable sensitivity with further scope of improvement. The Fig. 6.9 shows the time in advance the warnings were generated for approaching vehicles. It can be inferred that most of the warnings were generated between 5 and 6 seconds and only a very few were generated between 2 and 4 seconds with a lowest of 2.3 seconds. The warnings that were slight delayed were inferred to be due to the reduced detection range of relatively fast moving targets in noisy road scenarios. Most of these targets were seen to be bicycles. However, These results align very well with the configured threshold of 6 seconds and verify the performance of the warning system.

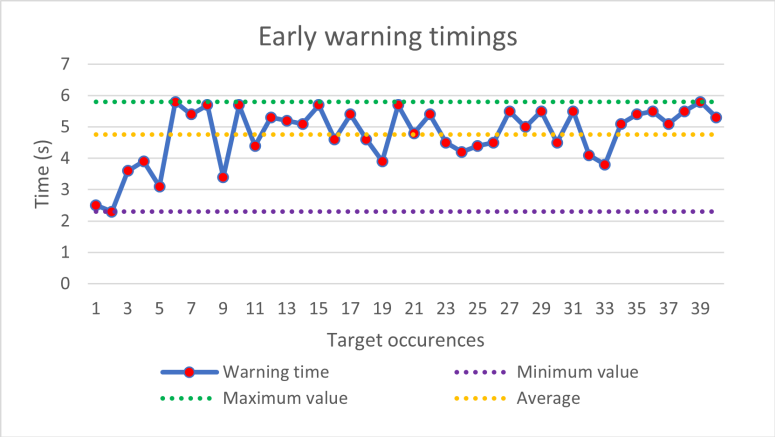

Figure 6.9: Early Warning Timings

6.4 Limitations

The benefits of using the proposed methods such longer detection range, higher early warning timings, higher accuracy, and mainly the ability to perform well across different real-road scenarios are evident from the results mentioned above. However, the system still has some limitations that need to be addressed in the future. One of the main limitation of the system was seen to be the reduced sensitivity of the system in all the road-scenarios as shown Table 6.5. This was mainly inferred to be due the maximum detection range configuration of the radar, the MSD setting for the threat assessment of the sides according to minimal lateral displacement scenarios to reduce the false warnings as mentioned in Section 5.2.2, and the high sampling rate of the system. These factors contribute to the inability of the system to effectively detect very close-by targets and generate warnings accordingly. To elaborate on the limitations let us consider a scenario of an approaching target at a lateral distance of 2m from the bicycle. The target is detected at a far distance and warnings are generated earlier, but when the target comes very close to the radar (longitudinal distance < 0.4m) it is not detected by the radar due to its reduced resolution. At this point in time the target is present within the coverage range of the ultrasonic sensor on the side considering its length, but a warning is not generated due to reduced MSD of 0.5m configured on the sides. These scenarios contribute to the FN of the system and increase by a factor of 2 every second due to the high sampling rate of the system. These are the reasons for the reduced sensitivity of the the system in noisy shared road scenarios, where the speed of the targets are relatively slower and the lateral distances of approaching target vehicles are higher, than dedicated bicycle lane scenarios. These limitation can be solved by two methods, one is

to reduce the sampling rate of the system, and the other is to vary the radar front-end configuration and the MSD for the sides according to the road scenario. The first method is more viable and easier to implement but may result in slightly delayed warnings and increased FP. Whereas the second method will be more accurate and effective, but will increase the complexity of the system as well as require a sensing method to differentiate road scenarios. A thorough analysis considering all these trade-off must be done in the future before addressing the limitations.

Chapter 7

Conclusion

In this thesis, an on-board early warning system for safe lateral maneuver of bicycle was designed and tested in real-road scenarios. Multi-modal off-the-shelf sensors like mmWave radar and ultrasonic sensor were used to extract information from the surrounding. The fusion of ultrasonic sensor and mmWave radar detects obstacles beyond the rider's peripheral vision and alerts only if the obstacle is a threat to the lateral maneuver. Both sensors measure the proximity of obstacles, while the mmWave radar also measures the relative velocity and the two-dimensional position of the obstacle relative to the radar that enables to compute the TTC and the direction of closing targets. Using these sensors, we estimate the TTC and MSD of the obstacle and deem its threat in a two-stage approach. The on-field testing in different real scenarios show that the system is robust in detecting true positives while minimizing false positives, with an overall accuracy of 95.2%. This proves that our system is not over-sensitive to non-threat obstacles. However, analyzing the sensitivity shows that the system is effective upto 73.7%. The reason for this limitation is addressed along with suggested methods to overcome them in Section 6.4. The results of the project are encouraging and has opened a new research direction for the implementation of lateral maneuver assistance systems in bicycles.

7.1 Future Work

There are a lot of features that can be added to this project to extend system functionality and improve its performance in the future. One such possibility for an adaptive system has already been mentioned in Section 6.4. The other possibility is to incorporate a suitable feedback mechanism to the host cyclist and the driver of the approaching targets based on the generated warning information. The feasibility of modifying the system to be triggered only when the cyclist initiates a lateral maneuver can be studied, as it is expected to reduce the power consumption and also reduce the generations of unnecessary warnings. Further extensive testing of the system across more complex traffic and road scenarios will provide more insight on further limitations of the system, that will lead to new research direction. An suitable housing to incorporate the system components without affecting the system performance must also be developed to evaluate the performance of the system across poor weather conditions such as rain. Designing a radar housing without deteriorating its performance by studying the permeability characteristics of the radar wave would be an ideal point to start. The radar EVM can be replaced with a custom designed board using only the IWR1642 sensor and necessary interfaces as it is inferred to be feasible.

Bibliography

[1] United Nations in Western Europe. *Cycling and Sustainable Development Goals*. https://unric.org/en/sustainable-development-goals-cycling/. [Online; accessed 7-August-2021].

[2] Iea. *Improving the sustainability of passenger and freight transport*. https://www.iea.org/topics/transport. [Online; accessed 7-August-2021].

[3] Cycling Industries Europe. *New European cycling industry forecast*. https://cyclingindustries.com/news/details/new-european-cycling-industry-forecast-shows-huge-growth-in-bike-and-e-bike-sales. [Online; accessed 11-November-2021].

[4] Lucas Harms and Maarten Kansen. *Cycling Facts*. https://www.government.nl/binaries/government/documents/reports/2018/04/01/cycling-facts-2018/Cycling+facts+2018.pdf. [Online; accessed 10-August-2021]. 2018.

[5] Statistics Netherlands. *Decline in road fatalities larger among motorists than cyclists*. https://www.cbs.nl/en-gb/news/2020/31/decline-in-road-fatalities-larger-among-motorists-than-cyclists. [Online; accessed 11-November-2021].

[6] Dutch Mobility Innovations. *The Netherlands is second place for cyclist deaths in Europe*. https://dutchmobilityinnovations.com/spaces/86/dutch-mobility-innovations/articles/news/30909/the-netherlands-is-second-place-for-cyclist-deaths-in-europe. [Online; accessed 11-November-2021].

[7] Xiangmo Zhao et al. "Fusion of 3D LIDAR and Camera Data for Object Detection in Autonomous Vehicle Applications". In: *IEEE Sensors Journal* 20.9 (2020), pp. 4901–4913.

[8] S. Ammoun and Fawzi Nashashibi. "Design and efficiency measurement of cooperative driver assistance system based on wireless communication devices". In: *Transportation Research Part C: Emerging Technologies* 18 (June 2010), pp. 408–428.

[9] Arne Bartels, Marc-Michael Meinecke, and Simon Steinmeyer. "Lane Change Assistance". In: *Handbook of Intelligent Vehicles*. Ed. by Azim Eskandarian. London: Springer London, 2012, pp. 729–757. ISBN: 978-0-85729-085-4.

[10] R. Dang et al. "A lane change warning system based on V2V communication". In: *17th International IEEE Conference on Intelligent Transportation Systems (ITSC)*. 2014, pp. 1923–1928.

[11] Q. Wu et al. “Research on Lane-Change Strategy With Real-Time Obstacle Avoidance Function”. In: *IEEE Access* 8 (2020), pp. 211255–211268.

[12] S. Sivaraman and M. M. Trivedi. “Dynamic Probabilistic Drivability Maps for Lane Change and Merge Driver Assistance”. In: *IEEE Transactions on Intelligent Transportation Systems* 15.5 (2014), pp. 2063–2073.

[13] Samyeul Noh and Kyounghwan An. “Risk assessment for automatic lane change maneuvers on highways”. In: *2017 IEEE International Conference on Robotics and Automation (ICRA)*. 2017, pp. 247–254.

[14] Robin Schubert, Karsten Schulze, and Gerd Wanielik. “Situation Assessment for Automatic Lane-Change Maneuvers”. In: *IEEE Transactions on Intelligent Transportation Systems* 11.3 (2010), pp. 607–616.

[15] S. Raviteja and R. Shanmughasundaram. “Advanced Driver Assistance System (ADAS)”. In: *2018 Second International Conference on Intelligent Computing and Control Systems (ICICCS)*. 2018, pp. 737–740.

[16] Stephen Smaldone et al. “Improving Bicycle Safety through Automated Real-Time Vehicle Detection”. In: (Sept. 2010).

[17] A. I. Alam et al. “IoT Enabled Smart Bicycle Safety System”. In: *2018 Joint 7th International Conference on Informatics, Electronics Vision (ICIEV) and 2018 2nd International Conference on Imaging, Vision Pattern Recognition (icIVPR)*. 2018, pp. 374–378.

[18] S. Kawanaka et al. “Approaching vehicle detection method with acoustic analysis using smartphone for elderly bicycle driver”. In: *2017 Tenth International Conference on Mobile Computing and Ubiquitous Network (ICMU)*. 2017, pp. 1–6.

[19] VanQuang Nguyen et al. “A Study on Real-Time Detection Method of Lane and Vehicle for Lane Change Assistant System Using Vision System on Highway”. In: *Engineering Science and Technology, an International Journal* 21.5 (2018), pp. 822–833. ISSN: 2215-0986.

[20] Javier Diaz Alonso et al. “Lane-Change Decision Aid System Based on Motion-Driven Vehicle Tracking”. In: *IEEE Transactions on Vehicular Technology* 57.5 (2008), pp. 2736–2746.

[21] Eui Yoon Chung et al. “Vision Based for Lane Change Decision Aid System”. In: *2006 International Forum on Strategic Technology*. 2006, pp. 10–13.

[22] R. P. Mahapatra et al. “Ultra Sonic Sensor Based Blind Spot Accident Prevention System”. In: *2008 International Conference on Advanced Computer Theory and Engineering*. 2008, pp. 992–995.

[23] Michail Papoutsidakis et al. “Motion Sensors and Transducers to Navigate an Intelligent Mechatronic Platform for Outdoor Applications”. In: *Sensors and Transducers* 198 (Apr. 2016), pp. 16–24.

[24] M. Klotz and H. Rohling. “24 GHz radar sensors for automotive applications”. In: *13th International Conference on Microwaves, Radar and Wireless Communications. MIKON - 2000. Conference Proceedings (IEEE Cat. No.00EX428)*. Vol. 1. 2000, 359–362 vol.1.

[25] Hui Zhang, Lin Li, and Ke Wu. "24GHz Software-Defined Radar System for Automotive Applications". In: *2007 European Conference on Wireless Technologies*. 2007, pp. 138–141.

[26] Yahya S. H. Khraisat. "Simulation of the 24GHz short range, wide band automotive radar". In: *11-th INTERNATIONAL RADAR SYMPOSIUM*. 2010, pp. 1–5.

[27] Vicentiu Cojocaru et al. "A 24GHz Low-Cost, Long-Range, Narrow-Band, Monopulse Radar Front End System for Automotive ACC Applications". In: *2007 IEEE/MTT-S International Microwave Symposium*. 2007, pp. 1327–1330.

[28] L. Wang G. Liu and S. Zou. *A radar-based blind spot detection and warning system for driver assistance*. 2017.

[29] Tomas Krejci and Michal Mandlik. "Close vehicle warning for bicyclists based on FMCW radar". In: *2017 27th International Conference Radioelektronika (RADIOELEKTRONIKA)*. 2017, pp. 1–5.

[30] Manfred Hägelen et al. "Safety and Comfort Enhancement with Radar for a Bicycle Assistance System". In: *2019 20th International Radar Symposium (IRS)*. 2019, pp. 1–7.

[31] Onur Toker and Suleiman Alsweiss. "mmWave Radar Based Approach for Pedestrian Identification in Autonomous Vehicles". In: *2020 SoutheastCon*. 2020, pp. 1–2.

[32] Masayuki Kishida, Katsuyuki Ohguchi, and Masayoshi Shono. "79 GHz-Band High-Resolution Millimeter-Wave Radar". In: *Fujitsu scientific & technical journal* 51 (Oct. 2015), pp. 55–59.

[33] Rekha Yadav, Pawan Kumar Dahiya, and Rajesh Mishra. "A high performance 76.5 GHz FMCW RADAR for advanced driving assistance system". In: *2016 3rd International Conference on Signal Processing and Integrated Networks (SPIN)*. 2016, pp. 383–388.

[34] A. Kawakubo et al. "Electronically-Scanning Millimeter-Wave RADAR for Forward Objects Detection". In: *SAE Transactions* 113 (2004), pp. 124–131. ISSN: 0096736X, 25771531.

[35] Yan Huang et al. "Density-Based Vehicle Detection Approach for Automotive Millimeter-Wave Radar". In: *2020 IEEE 3rd International Conference on Electronic Information and Communication Technology (ICEICT)*. 2020, pp. 534–537.

[36] Nikolaos Baras et al. "Autonomous Obstacle Avoidance Vehicle Using LIDAR and an Embedded System". In: *2019 8th International Conference on Modern Circuits and Systems Technologies (MOCAST)*. 2019, pp. 1–4.

[37] Abhir Naik et al. "LiEBiD - A LIDAR based Early Blind Spot Detection and Warning System for Traditional Steering Mechanism". In: *2020 International Conference on Smart Electronics and Communication (ICOSEC)*. 2020, pp. 604–609.

[38] Mohammad Ammar Bharmal and Muhammad H. Rashid. “Designing an Autonomous Cruise Control System using an A3 LIDAR”. In: *2019 2nd International Conference on Innovation in Engineering and Technology (ICIET)*. 2019, pp. 1–6.

[39] Cibby Pulikkaseril and Stanley Lam. “Laser Eyes for Driverless Cars: The Road to Automotive LIDAR”. In: *2019 Optical Fiber Communications Conference and Exhibition (OFC)*. 2019, pp. 1–4.

[40] Masaru Yoshioka et al. “Real-time object classification for autonomous vehicle using LIDAR”. In: *2017 International Conference on Intelligent Informatics and Biomedical Sciences (ICIIBMS)*. 2017, pp. 210–211.

[41] Mingguo Zhao, Sotirios Stasinopoulos, and Yongchao Yu. “Obstacle detection and avoidance for autonomous bicycles”. In: *2017 13th IEEE Conference on Automation Science and Engineering (CASE)*. 2017, pp. 1310–1315.

[42] Huawei. *Internet of Vehicles*. https://www.huawei.com/mediafiles/CORPORATE/PDF/Magazine/WinWin/HW_110848.pdf. [Online; accessed 11-November-2021].

[43] W. Yang, B. Wan, and X. Qu. “A Forward Collision Warning System Using Driving Intention Recognition of the Front Vehicle and V2V Communication”. In: *IEEE Access* 8 (2020), pp. 11268–11278.

[44] Michael Jenkins, Daniel Duggan, and Alessandro Negri. “Towards a connected bicycle to communicate with vehicles and infrastructure : Multimodel alerting interface with Networked Short-Range Transmissions (MAIN-ST)”. In: Mar. 2017, pp. 1–3.

[45] Ruina Dang et al. “Coordinated Adaptive Cruise Control System With Lane-Change Assistance”. In: *IEEE Transactions on Intelligent Transportation Systems* 16.5 (2015), pp. 2373–2383.

[46] M. B. Younes and A. Boukerche. “A vehicular network based intelligent lane change assistance protocol for highways”. In: *2017 IEEE International Conference on Communications (ICC)*. 2017, pp. 1–6.

[47] Le Liang et al. “Vehicular Communications: A Physical Layer Perspective”. In: *IEEE Transactions on Vehicular Technology* PP (Apr. 2017).

[48] SamYong Kim et al. “Front and rear vehicle detection and tracking in the day and night times using vision and sonar sensor fusion”. In: *2005 IEEE/RSJ International Conference on Intelligent Robots and Systems*. 2005, pp. 2173–2178.

[49] Y. Wei et al. “Vehicle Frontal Collision Warning System based on Improved Target Tracking and Threat Assessment”. In: *2007 IEEE Intelligent Transportation Systems Conference*. 2007, pp. 167–172.

[50] Heong-tae Kim and Bongsob Song. “Vehicle recognition based on radar and vision sensor fusion for automatic emergency braking”. In: *2013 13th International Conference on Control, Automation and Systems (ICCAS 2013)*. 2013, pp. 1342–1346.

[51] Jihun Kim, Dong Seog Han, and Benaoumeur Senouci. "Radar and Vision Sensor Fusion for Object Detection in Autonomous Vehicle Surroundings". In: *2018 Tenth International Conference on Ubiquitous and Future Networks (ICUFN)*. 2018, pp. 76–78.

[52] Micaela Verucchi et al. "Real-Time clustering and LiDAR-camera fusion on embedded platforms for self-driving cars". In: *2020 Fourth IEEE International Conference on Robotic Computing (IRC)*. 2020, pp. 398–405.

[53] C. Degen et al. "Driver Assistance System for Pedelecs". In: *2019 20th International Radar Symposium (IRS)*. 2019, pp. 1–8.

[54] John Dahl et al. "Collision Avoidance: A Literature Review on Threat-Assessment Techniques". In: 4 (Dec. 2018), pp. 101–113.

[55] J. Hillenbrand, K. Kroschel, and V. Schmid. "Situation assessment algorithm for a collision prevention assistant". In: *IEEE Proceedings. Intelligent Vehicles Symposium, 2005.* 2005, pp. 459–465.

[56] Sanhita Das and Akhilesh Kumar Maurya. "Time Headway Analysis for Four-Lane and Two-Lane Roads". In: *Transportation in Developing Economies* 3.1 (Apr. 2017), p. 9. ISSN: 2199-9295.

[57] Yizhen Zhang, Erik Antonsson, and K. Grote. "A new threat assessment measure for collision avoidance systems". In: Oct. 2006, pp. 968–975.

[58] László Pokorádi. "Fuzzy logic-based risk assessment". In: *Academic and Applied Research in Military Science* 1 (Jan. 2002).

[59] Takashi Wakasugi. *A study on warning timing or lane change decision aid systems based on driver's lane change maneuver.*

[60] Sandeep Rao. *Introduction to mmwave Sensing: FMCW Radars.* https://training.ti.com/sites/default/files/docs/mmwaveSensing-FMCW-offlineviewing_4.pdf. [Online; accessed 11-November-2021].

[61] Elementz Online. *Ultrasonic Sensor HC-SR04 with Arduino.* https://www.elementzonline.com/blog/ultrasonic-sensor-hc-sr04-with-arduino. [Online; accessed 11-November-2021].

[62] Texas Instruments. *IWR1642 Evaluation Module.* https://www.ti.com/lit/ug/swru521c/swru521c.pdf?ts=1636541979958&ref_url=http. [Online; accessed 9-August-2021].

[63] Andrzej Wojtkiewicz et al. "Two-dimensional Signal Processing in FMCW Radars". In: Oct. 1997.

[64] Christina Katzlberger. "Object Detection with Automotive Radar Sensors using CFAR Algorithms". In: 2018.

[65] Domenic Belgiovane and Chi-Chih Chen. "Bicycles and human riders backscattering at 77 GHz for automotive radar". In: *2016 10th European Conference on Antennas and Propagation (EuCAP)*. 2016, pp. 1–5.

[66] Martin Ester et al. "A Density-Based Algorithm for Discovering Clusters in Large Spatial Databases with Noise". In: *Proceedings of the Second International Conference on Knowledge Discovery and Data Mining*. KDD'96. Portland, Oregon: AAAI Press, 1996, pp. 226–231.

[67] Apple. *Measure Application*. https://support.apple.com/en-us/HT208924. [Online; accessed 11-September-2021].

[68] Bol. *Walfort Wireless Bicycle Computer Cycle Computer - Wireless*. https://www.bol.com/nl/nl/p/walfort-wireless-bicycle-computer-fietscomputer-draadloos/9300000001595055/. [Online; accessed 11-November-2021].